

Journal of
Mechanics of
Materials and Structures

**NONLINEAR BEHAVIOR OF THERMALLY LOADED CURVED
SANDWICH PANELS WITH A TRANSVERSELY FLEXIBLE CORE**

Yeoshua Frostig and Ole Thomsen

Volume 4, N° 7-8

September 2009

 mathematical sciences publishers

NONLINEAR BEHAVIOR OF THERMALLY LOADED CURVED SANDWICH PANELS WITH A TRANSVERSELY FLEXIBLE CORE

YEOSHUA FROSTIG AND OLE THOMSEN

The nonlinear analysis of a curved sandwich panel with a compliant core subjected to a thermal field and mechanical load is presented. The mathematical formulation is developed first, along with the solution of the stress and displacement fields for the case of a sandwich core with mechanical properties that are independent of the temperature. The nonlinear analysis includes geometrical nonlinearities in the face sheets caused by rotation of the face cross sections and high-order effects due to the transversely flexible core. The mathematical formulation uses the variational principle of minimum energy along with HSAPT (high-order sandwich panel theory) to derive the nonlinear field equations and the boundary conditions. The full displacement and stress fields of the core with uniform temperature-independent mechanical properties and the appropriate governing equations of the sandwich panel are given.

This is followed by the general solution of the core stress and displacement fields when the mechanical core properties are dependent on the radial (through-the-thickness) coordinate. The displacement fields of a core with temperature-dependent mechanical properties are determined explicitly using an equivalent polynomial description of the varying properties.

A numerical study then describes the nonlinear response of curved sandwich panels subjected to concentrated and distributed mechanical loads, thermally induced deformations, and simultaneous thermal and mechanical loads where the mechanical load is below the limit load level of the mechanical response and the imposed temperature field is made to vary. The results reveal that the thermomechanical response is linear when the sandwich panel is heated, but becomes nonlinear with limit point behavior when the panel is cooled down.

Introduction

Curved sandwich structures are increasingly being used in the aerospace, naval and transportation industries, where weight savings combined with high strength and stiffness properties are always in demand. Sandwich structures consist of two thin face sheets, usually metallic or laminated composites, bonded to a core that is often made of honeycomb or a polymer foam with low strength properties. The core usually provides the shear resistance/stiffness to the sandwich structure in the transverse (radial) direction, and a transverse support to the face sheets that is associated to radial normal stresses. Polymer foam or low-strength honeycomb cores are flexible in this (radial/thickness) direction, and this affects both the global and the local response through changes of the core height (compressible core), and a core cross section plane that deforms into a nonlinear pattern.

The manufacture of such sandwich structures often involves elevated temperatures that may be associated with thermally induced deformations. During service, deformations may be induced by elevated

Keywords: sandwich structures, thermal effects, nonlinear geometry, softcore, high-order models.

temperatures, with or without large gradients, which may degrade the properties of the face sheets and the core. In a traditional design process of such structures the thermally induced deformations and the deformations caused by external mechanical loads are considered separately. However, this approach is not necessarily conservative, since the interaction between the external loads and the elevated temperatures, especially when the deformations are large, may lead to unsafe behavior and loss of structural integrity.

The major goal of this work is to investigate under what circumstances the combination of simultaneous thermally induced deformations and mechanical loads applied to curved sandwich structures (panels) may lead to an unstable and thereby potentially disastrous load response.

Outline. After a discussion of earlier work in Section 1 we introduce in Section 2 the mathematical formulation leading to the field and governing equations, the appropriate boundary conditions, the thermal fields within the core, along with the effects of the degradation of the mechanical core properties as a result of elevated temperatures. The full nonlinear governing equations for the temperature-independent (TI) case are derived and presented in Section 3. In Section 4 we turn to the general solution for the core stress and displacement fields when the core properties are coordinate-dependent in the radial (through-the-thickness) direction and display mechanical properties that are temperature-dependent (TD). This is followed in Section 5 by a numerical investigation into the nonlinear response of sandwich panels; the results are described in Section 5.1 for TI cores and in Section 5.2 for TD cores. Further discussion of the numerical study and overall conclusions occupy Section 6.

1. Antecedents

The well known approach for sandwich plates/panels, due to Reissner and Mindlin, replaces the layered sandwich panel by an equivalent single layer (ESL) and takes into the account the relaxed Kirchhoff–Love hypothesis, which assumes that the section plane is not normal to the plate middle surface. This approach has become the foundation for a large group of research works in the field of sandwich structures, including [Whitney and Pagano 1970; Noor and Burton 1990; Noor et al. 1994; 1996], to name a few; see also the references listed in this last paper. Kollár [1990] investigated buckling of generally anisotropic shallow sandwich shells and Vaswani et al. [1988] performed vibration and damping analysis of curved sandwich beams. These last two models used the Flügge shell theory while assuming that the face sheets are membranes and the core is incompressible. A model for shallow cylindrical sandwich panels with orthotropic surfaces suggested in [Wang and Wang 1989] follows the same relaxed Kirchhoff–Love hypothesis for the core as in references quoted above, but in this work the face sheets are attributed with both in-plane and flexural rigidities. Similarly, using the principle of virtual work along with the Reissner–Mindlin hypothesis and Sanders’ nonlinear stress-displacement relations, a theory for thick shells has been developed [di Sciuva 1987; di Sciuva and Carrera 1990] that takes into account the shear rotation but assumes that the core is incompressible and linear. A stability analysis for cylindrical sandwich panels with laminated composite faces based on the Reissner hypothesis has been derived [Rao 1985; Rao and Meyer-Piening 1986; 1990]. These authors extended the Reissner–Mindlin theory to derive force-displacement relations of anisotropic sandwich panels with membrane face sheets. As a consequence, local effects, due to localized loads, point supports, presence of load or geometric discontinuities are beyond the capability of these approaches. This well known approach is accurate as long as the core can be considered to be incompressible, i.e., the height of the core remains unchanged so the radial

displacements of the two face sheets are identical. However, compliant core materials such as relatively soft polymer foams are used in many modern sandwich structures. Accordingly it is necessary to relax the Reissner–Mindlin constraints to account for localized effects caused by the change of core height during the deformation of the sandwich structure considered.

A class of high-order theories based on the assumption of cubic and quadratic or trigonometric through-the-thickness distributions for the displacements have been suggested in [Lo et al. 1977; Librescu and Hause 2000; Stein 1986; Reddy 1984a; 1984b]. The results usually include terms that have no physical meaning due to the integration through the thickness. Lo et al. [1977] assumed a cubic shape for the in-plane deformations and a quadratic distribution for the vertical deformation. Stein [1986] used trigonometric series for the displacement distributions. Reddy [1984a; 1984b] also assumed cubic distributions for the in-plane displacements whereas the vertical displacement is assumed to be uniform across the thickness. In addition, the condition of zero shear stresses at the outer fibers of the section was also adopted. All the referenced high-order models use integration through the thickness along with variational principle and in general they are valid for sandwich panels with an incompressible core.

Many investigators have performed numerical analyses of the overall behavior of curved sandwich panels using FEA; see for example [Hildebrand 1991; Hentinen and Hildebrand 1991; Smidt 1995; 1993; Tolf 1983; Kant and Kommineni 1992]. The different analyses, linear or nonlinear, use various types of finite elements along with the limiting Reissner–Mindlin hypothesis, thus ignoring localized effects.

A different approach that includes the effect of the transverse (radial) normal stresses on the overall behavior of sandwich shells has been considered by Kühhorn and Schoop [1992], who introduced geometrically nonlinear kinematic relations along with pre-assumed polynomial deformation patterns for plates and shells. In recent years, the effects of incorporating a vertical flexible core on the local and overall behavior of the flat and curved sandwich panels have been implemented through the use of the high-order theory (HSAPT); see [Frostig et al. 1992] for flat panels, [Bozhevolnaya and Frostig 1997] for nonlinear behavior, [Bozhevolnaya 1998] on shallow sandwich panels, [Karayadi 1998] on cylindrical shells, [Frostig 1999] on the linear behavior of curved sandwich panels, [Bozhevolnaya and Frostig 2001] on the free vibration of curved panels, and [Thomsen and Vinson 2001] on composite sandwich aircraft fuselage structures.

Thermal effects in curved sandwich panels have been considered in [Noor et al. 1997] using a first-order shear deformation computation model with incompressible core. A thermomechanical FE analysis was conducted by Ko [1999], who looked into the peeling stresses involved at the face-core interfaces under cryogenic bending loading conditions. Librescu et al. [1994; 2000] investigated the thermomechanical response of flat and curved panels using a high-order theory that includes transverse (radial) shear flexibility but ignoring the transverse (radial) flexibility of the core. Fernlund [2005] used a simplified sandwich model that ignores the radial stresses as well as the shear deformation in the core in order to determine the spring-in effects of angled sandwich panels.

The thermal and the thermomechanical nonlinear response of a flat sandwich panel with a compressible core has been considered in [Frostig and Thomsen 2008a; 2008b], along with the effect of the thermal degradation of the mechanical properties of the core; see [Frostig and Thomsen 2007]. This series of papers reveals that the transverse flexibility of the core along with its extension and compression as a result of the thermally induced deformation play a major role in the nonlinear response of sandwich panels.

2. Mathematical formulation

The mathematical formulation presented in the paper uses high-order sandwich panel theory (HSAPT) to model the nonlinear response of a curved sandwich panel when subjected to thermally induced deformation along with mechanical loads. The sandwich panel is modeled as two curved faces, with membrane and flexural rigidities following the Euler–Bernoulli hypothesis, that are interconnected through compatibility and equilibrium with a two-dimensional compliant (compressible or extensible) elastic core with shear and radial (through-the-thickness) normal stress resistance. The HSAPT model for the curved panel adopts the following restrictive assumptions:

- The face sheets have in-plane (circumferential) and bending rigidities with small moderate deformations class of kinematic relation [Brush and Almroth 1975; Simites 1976] and negligible shear deformations.
- The core is considered as a two-dimensional linear elastic continuum obeying small deformation kinematic relations; the core height may change and the section planar does not remain plane after deformation.
- The core is assumed to possess shear and radial normal stiffness only, and the in-plane (circumferential) normal stiffness is assumed negligible. Accordingly, the circumferential normal stresses are assumed to be nil.
- Full bonding between the face sheets and the core is assumed and the interfacial layers can resist shear as well as radial normal stresses.
- The loads are applied to the face sheets only.

Field equations and boundary conditions. The field equations and the boundary conditions are derived following the steps of the HSAPT approach for the curved sandwich panel [Frostig 1999; Bozhevolnaya and Frostig 1997]. The field equations are derived using the variational principle of extremum of the total potential energy:

$$\delta(U + V) = 0, \quad (1)$$

where δ is the variational operator, U is in the internal potential strain energy and V is the external potential energy.

The internal potential energy of a fully bonded panel in terms of polar coordinates reads

$$\begin{aligned} \delta U = & \int_0^a \int_{-\frac{1}{2}d_j}^{\frac{1}{2}d_j} \int_{-\frac{1}{2}b_w}^{\frac{1}{2}b_w} \sigma_{sst}(\phi, z_t) \delta \epsilon_{sst}(\phi, z_t) r_t dy dz_t d\phi \\ & + \int_0^a \int_{-\frac{1}{2}d_b}^{\frac{1}{2}d_b} \int_{-\frac{1}{2}b_w}^{\frac{1}{2}b_w} \sigma_{ssb}(\phi, z_b) \delta \epsilon_{ssb}(\phi, z_b) r_b dy dz_b d\phi \\ & + \int_0^a \int_{r_{bc}}^{r_{tc}} \int_{-\frac{1}{2}b_w}^{\frac{1}{2}b_w} (\tau_{rs}(\phi, r_c) \delta \gamma_{rs}(\phi, r_c) + \sigma_{rr}(\phi, r_c) \delta \epsilon_{rr}(\phi, r_c)) r_c dy dr_c d\phi, \end{aligned} \quad (2)$$

where $\sigma_{ssj}(\phi, r_j)$ and $\epsilon_{ssj}(\phi, r_j)$ ($j = t, b$) are the stresses and strains, respectively, in the circumferential directions of the face sheets; $\tau_{rs}(\phi, r_c)$ and $\gamma_{rs}(\phi, r_c)$ are the shear stresses and strains; $\sigma_{rr}(\phi, r_c)$ and $\epsilon_{rr}(\phi, r_c)$ are the radial normal stresses and strains; r and s refer to the radial and circumferential

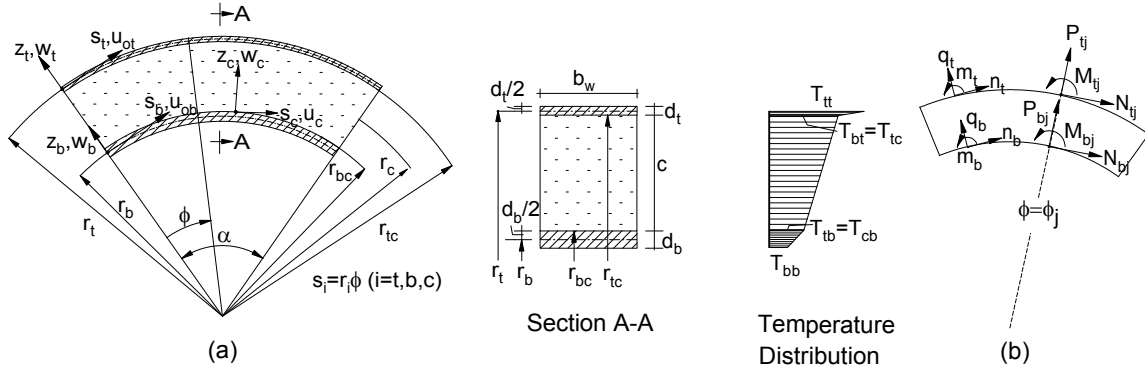


Figure 1. Dimensions, temperature distribution and sign conventions for a curved sandwich panel: (a) geometry; (b) loads at face sheets.

directions of the curved panel; α is the total angle of the curved panel; r_j ($j = t, b, c$) denote the radii of the centroidal lines of the top and both face sheets and the core; $r_{tc} = r_t - d_t/2$ and $r_{bc} = r_b + d_b/2$ refer to the radii of the upper and lower interface line; b_w is the width and d_j ($j = t, b$) are the thicknesses of the face sheets. For geometry, sign conventions, coordinates, deformations and internal resultants, see Figure 1.

The variation of the external energy reads

$$\delta V = - \int_{s=0}^L (n_t \delta u_{ot} + q_t \delta w_t - m_t \delta \beta_t) ds_t - \int_{s=0}^L (n_b \delta u_{ob} + q_b \delta w_{bt} - m_b \delta \beta_b) ds_b - \sum_{j=t,b} \sum_{i=1}^{NC_j} \int_{s=0}^L (N_{ij} \delta u_{oj} + P_{ij} \delta w_j - M_{ij} \delta \beta_j) \delta_d(s_j - s_{it}) ds_j, \tag{3}$$

where n_j , q_j and m_j ($j = t, b$) are the external distributed loads in the circumferential and radial directions, respectively, and the distributed bending moment applied at the face sheets; u_{oj} and w_j ($j = t, b$) are the circumferential and radial displacements of the face sheets, respectively; β_j is the slope of the section of the face sheet; N_{eij} , P_{eij} and M_{eij} ($j = t, b$) are the concentrated external loads in the circumferential and radial directions, respectively, and the concentrated bending moment applied at either face sheet at $s = s_{ij}$; NC_j ($j = t, b$) is the number of concentrated loads at the top and bottom faces, and $\delta_d(s_j - s_{ji})$ is the Dirac function at the location of the concentrated loads. For sign conventions and definition of loads see Figure 1.

The displacement pattern of the face sheets through their depth follows the Euler–Bernoulli assumptions with negligible shear strain and kinematic relations of small deformation and they read, for $j = t, b$,

$$u_j(\phi, z_j) = u_{oj}(\phi) + z_j \beta_j(\phi), \quad \beta_j(\phi) = \frac{1}{r_j} u_{oj}(\phi) - \frac{1}{r_j} \frac{d}{d\phi} w_j(\phi), \tag{4}$$

where z_j is the radial coordinate measured *upward* from the centroid of each face sheet, r_j is the radius and $s_j = r_j \phi$ is the circumferential coordinate of the face sheets, which have identical radial center, and ϕ is the angle measured from the origin; see Figure 1 for the geometry. Hence, the strain distribution is

also assumed to be linear and it reads

$$\varepsilon_{ssj}(\phi) = \varepsilon_{ossj}(\phi) + z_j \chi_j(\phi), \tag{5}$$

where the mid-plane strain and the curvature equal

$$\varepsilon_{ossj}(\phi) = \frac{d}{d\phi} u_{oj}(\phi) + \frac{w_j(\phi)}{r_j(\phi)} + \frac{1}{2} \beta_j(\phi)^2, \quad \chi_j(\phi) = \frac{1}{r_j} \frac{d}{d\phi} \beta_j(\phi) = \frac{1}{r_j^2} \frac{d}{d\phi} u_{oj}(\phi) - \frac{1}{r_j^2} \frac{d^2}{d\phi^2} w_j(\phi). \tag{6}$$

Notice that thermal strains do not appear in the terms of the strains of the face sheets.

The kinematic relations for the core, under the approximation of small deformations, read

$$\varepsilon_{rrc}(\phi, r) = \frac{\partial}{\partial r} w_c(\phi, r), \quad \gamma_c(\phi, r) = \frac{\partial}{\partial r} u_c(\phi, r) - \frac{u_c(\phi, r)}{r} + \frac{1}{r} \frac{\partial}{\partial \phi} w_c(\phi, r), \tag{7}$$

where $w_c(\phi, r)$ and $u_c(\phi, r)$ are the radial and circumferential displacements of the core, respectively.

The compatibility conditions corresponding to perfect bonding between the face sheets and the core require that

$$u_c(\phi, r = r_{jc}) = u_{oj}(\phi) - \frac{\lambda}{2r_j} d_j(u_{oj}(\phi) - w_j(\phi), \phi), \quad w_c(\phi, r = r_{jc}) = w_j(\phi), \tag{8}$$

where $\lambda = 1, -1$ for $j = t, b$, respectively; r_{jc} ($j = t, b$) are the radii of the upper and lower face-core interfaces; and $u_c(r = r_{jc}, \phi)$, $w_c(r = r_{jc}, \phi)$ are the displacements of the core in the circumferential and radial directions at the face-core interfaces.

The field equations and the boundary conditions are derived using the variational principle (1), the variational expressions (2) and (3) of the energies, the kinematic relations (5)–(7) of the face sheets and the core, the compatibility requirements (8), and the stress resultants. See Figure 2.

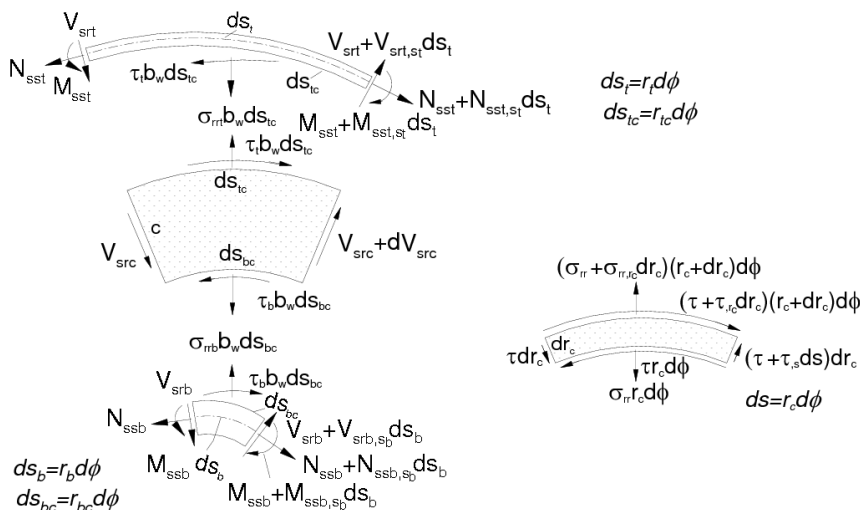


Figure 2. Internal stress resultants and stresses within a curved sandwich panel segment. Left: stress resultants on the deformed shape of the panel. Right: stresses within the core.

The field equations, after integration by parts and some algebraic manipulations, read as follows (notice that since the strains in the core are linear, the field equations of the core coincide with those for the geometrically linear case [Frostig 1999] and are presented here only for convenience):

Face sheets ($j = t, b$):

$$\begin{aligned} &\left(-\frac{d_j}{2r_j} + \lambda\right)b_w r_{jc} \tau_{sr}(\phi, r = r_{jc}) + \frac{1}{r_j} \left(u_{oj}(\phi) - \frac{dw_j(\phi)}{d\phi}\right) N_{ssj}(\phi) - \frac{dN_{ssj}(\phi)}{d\phi} \\ &\qquad\qquad\qquad + m_j(\phi) - \frac{1}{r_j} \frac{dM_{ssj}(\phi)}{d\phi} - r_j n_j = 0, \\ &\left(1 + \frac{1}{r_j} \left(\frac{du_{oj}(\phi)}{d\phi} - \frac{d^2 w_j(\phi)}{d\phi^2}\right)\right) N_{ssj}(\phi) + \frac{1}{r_j} \left(u_{oj}(\phi) - \frac{dw_j(\phi)}{d\phi}\right) \frac{dN_{ssj}(\phi)}{d\phi} \\ &\qquad + \lambda b_w r_{jc} \sigma_{rr}(\phi, r = r_{jc}) - \frac{b_w d_j r_{jc}}{2r_j} \frac{d\tau_{sr}(\phi, r = r_{jc})}{d\phi} - \frac{1}{r_j} \frac{d^2 M_{ssj}(\phi)}{d\phi^2} + \frac{dm_j(\phi)}{d\phi} - r_j q_t = 0. \end{aligned} \tag{9}$$

Core:

$$r_c \frac{\partial \tau_{sr}(\phi, r_c)}{\partial r_c} + 2\tau_{sr}(\phi, r_c) = 0, \qquad r_c \frac{\partial \sigma_{rr}(\phi, r_c)}{\partial r_c} + \sigma_{rr}(\phi, r_c) + \frac{\partial \tau_{sr}(\phi, r_c)}{\partial \phi} = 0. \tag{10}$$

Here N_{ssj} and M_{ssj} ($j = t, b$) are the in-plane and bending moment stress resultants of each face sheet; $\tau_{sr}(\phi, r = r_{jc})$ and $\sigma_{rr}(\phi, r = r_{jc})$ (with $j = t, b$) are the shear and vertical normal stresses, respectively, at the face-core interfaces; and $\lambda = 1, -1$ for $j = t, b$. Notice that here the nonlinear terms involve also in-plane displacements, unlike the case of flat panels. Note also that, due to the geometrical nonlinearities of the face sheets, the equilibrium conditions, which are described by the field equations, correspond to the deformed shape of the face sheets and the undeformed shape of the core; see Figure 2.

Boundary conditions for the curved sandwich panel where the loads and constraints are defined in the circumferential and radial directions of each face sheet and the core independently are called local boundary conditions; see Figure 3(a) on the next page. These conditions at $\phi_e = 0, \alpha$ read as follows:

Face sheets ($j = t, b$):

$$\begin{aligned} &\lambda \left(\frac{M_{ssj}(\phi_e)}{r_j} + N_{ssj}(\phi_e) \right) - N_{ej} + \frac{M_{ej}}{r_j} = 0 \quad \text{or} \quad u_{oj}(\phi_e) = u_{eoj}, \\ &\qquad\qquad\qquad \lambda \frac{M_{ssj}(\phi_e)}{r_j} + \frac{M_{ej}}{r_j} = 0 \quad \text{or} \quad w_{j,\phi}(\phi_e) = Dw_{ej}, \\ &\lambda \left(\frac{D(w_j)(\phi_e) - u_{oj}(\phi_e)}{r_j} N_{ssj}(\phi_e) + \frac{D(M_{ssj})(\phi_e)}{r_j} \right. \\ &\qquad\qquad\qquad \left. - m_j(\phi_e) + \frac{b_w d_j r_{jc} \tau_j(\phi_e)}{2r_j} \right) - P_{ej} = 0 \quad \text{or} \quad w_j(\phi_e) = w_{ej}, \end{aligned} \tag{11}$$

where $\lambda = 1$ for $\phi_e = \alpha$ and $\lambda = -1$ for $\phi_e = 0$, in all three equations; u_{eoj} , w_{ej} are the prescribed circumferential and radial displacements at the edges of the face sheets; Dw_{ej} is the rotation at the same edges; and N_{ej} , P_{ej} , M_{ej} are the imposed external loads. Notice that the circumferential force condition (the first of the three equations above) is actually a combined stress resultant that results from a moment equilibrium about the radial center of the face sheet.

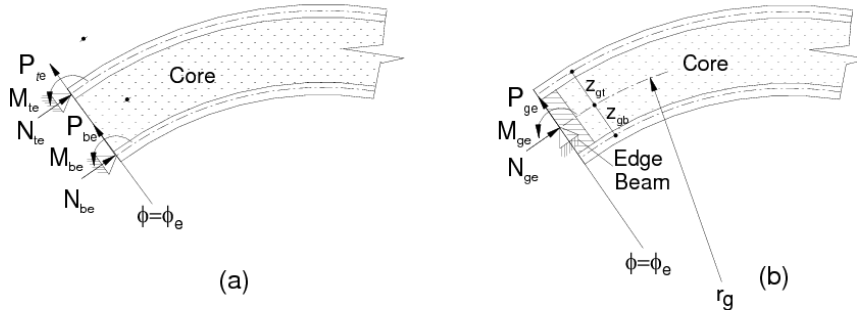


Figure 3. Edge conditions at the edge of a curved sandwich panel: (a) conventional edge with isolated supports; (b) reinforced edge with an edge beam.

Core: The boundary conditions at $\phi_e = 0, \alpha$, through the depth of the core, at $r_{bc} \leq r_c \leq r_{tc}$, read

$$\tau_{rs}(\phi_e, r_c) = 0 \quad \text{or} \quad w_c(\phi_e, r_c) - w_{ec}(r_c) = 0, \tag{12}$$

where $w_{ec}(r)$ denotes the prescribed deformations at the ends of the sandwich panel.

For the case where an edge beam connects the two face sheets and the core, the two face sheets undergo identical displacements and rotations; see Figure 3(b). Thus the distribution of the displacement through the depth of the sandwich panel follows those of a face sheet, given in (4):

$$u_g(\phi_e, z_g) = u_{go}(\phi_e) + \frac{z_g}{r_g} (u_{go}(\phi_e) - D(w_g)(\phi_e)), \tag{13}$$

where $u_{go}(\phi_e)$ denotes the circumferential displacements and $D(w_g)(\phi_e)$ the rotation of the centroid line of the section with the edge beam; see again Figure 3(b). In order to use these displacements, denoted as global displacements, in the variational terms of the boundary conditions that result from the partial integration of the internal and external potential energy terms and the contribution of the loads at the edges of the panel, the global in-plane displacements and rotations must be defined in terms of the displacements and rotation of the face sheets. Hence, these unknowns are determined by imposing the conditions that the global displacements $u_g(\phi_e, z_g)$ at the centroid of the upper and lower face sheets must equal the in-plane displacements $u_{oj}(\phi_e)$ of the face sheets. Thus they read

$$D(w_g)(\phi_e) = \frac{r_t u_{ob}(\phi_e) + r_b u_{ot}(\phi_e)}{c + \frac{1}{2}d_t + \frac{1}{2}d_b}, \quad u_{go}(\phi_e) = \frac{z_{gb} u_{ot}(\phi_e) + z_{gt} u_{ob}(\phi_e)}{c + \frac{1}{2}d_t + \frac{1}{2}d_b}. \tag{14}$$

The existence of the edge beam also imposes relations between the displacements of the face sheets:

$$w_t(\phi_e) = w_b(\phi_e), \quad \beta_t(\phi_e) = \beta_b(\phi_e), \quad \beta_t(\phi_e) = \frac{u_{ot}(\phi_e) - u_{ob}(\phi_e)}{z_{eb} + z_{et}}, \tag{15}$$

where the last equality results from the requirement that the slope of the section of the face sheets and that of the edge beam must be identical.

The global boundary conditions are derived by expressing the displacements and rotations of the face sheets in terms of the global displacements using (14) and (15), and substituting them into the variational

terms at the edges. Hence, by collecting terms with respect to the in-plane displacement and rotation of the edge beam, one obtains for these global conditions

$$\begin{aligned} \frac{r_t N_{sst}(\phi_e) + M_{ssb}(\phi_e) + M_{sst}(\phi_e) + r_b N_{ssb}(\phi_e) + M_{ge}(\phi_e)}{r_g} - N_{ge}(\phi_e) &= 0 \quad \text{or} \quad u_{go}(\phi_e) = u_{geo}, \\ -N_{sst}(\phi_e) z_{gt} - M_{ssb}(\phi_e) - M_{sst}(\phi_e) + N_{ssb}(\phi_e) z_{gb} - M_{ge}(\phi_e) &= 0 \quad \text{or} \quad D(w_g)(\phi_e) = D w_{ge}, \\ V_{srt}(\phi_e) + V_{srb}(\phi_e) + \frac{b_w r_{tc} (r_{tc} - r_{bc}) \tau_t(\phi_e)}{r_{bc}} - P_{ge} &= 0 \quad \text{or} \quad w_g(\phi_e) = w_{ge}, \end{aligned} \tag{16}$$

where $V_{srj}(\phi)$ ($j = t, b$) is the radial shear stress resultant in each of the face sheets, which equals

$$V_{srj}(\phi_e) = \frac{D(w_j)(\phi_e) - u_{oj}(\phi_e)}{r_j} N_{ssj}(\phi_e) + \frac{D(M_{ssj})(\phi_e)}{r_j} + \frac{b_w d_j r_{jc} \tau_{sr}(\phi_e, r = r_{jc})}{2r_j} - m_j(\phi_e). \tag{17}$$

Under the assumption of a perfect bond between the edge beam and the core (through the full core depth) the radial displacement field of the core must be uniform through its depth. This is possible only when the upper and lower face sheets have identical displacements; see (15). This is equivalent to a weaker version of the requirement (12)₂, namely

$$w_c(\phi_e) \approx \frac{1}{c} \int_{r_{bc}}^{r_{tc}} w_c(\phi_e, r_c) dr_c = w_{ge}(\phi_e). \tag{18}$$

3. Governing equations in the temperature-independent case

To determine the governing equations we must first define the stress and displacement fields of the core.

Core displacement and stress fields: uniform mechanical properties (TI). The explicit descriptions of the stress and displacement fields of the core are determined through the compatibility conditions (8), applied to the following constitutive relations of an isotropic core:

$$\varepsilon_{rr}(\phi, r_c) = \frac{\sigma_{rr}(\phi, r_c)}{E_{rc}} + \alpha_{Tc} T_c(r_c, \phi), \quad \gamma_{sr}(\phi, r_c) = \frac{\tau_{sr}(\phi, r_c)}{G_{src}}, \tag{19}$$

where T_c is the temperature function and E_{rc}, G_{src} are the Young's and shear moduli of the core in the radial direction.

The stress fields within the core are derived through the solution of the field equations (10) of the core, which reads

$$\begin{aligned} \tau_{sr}(\phi, r_c) &= \frac{r_{tc}^2}{r_c^2} \tau_t(\phi), \quad \sigma_{rr}(\phi, r_c) = \frac{r_{tc}^2}{r_c^2} \frac{d\tau_t(\phi)}{d\phi} + \frac{C_{w1}(\phi)}{r_c}, \quad \tau_b(\phi) = \frac{r_{tc}^2}{r_{bc}^2} \tau_t(\phi), \\ \sigma_{rrj}(\phi) &= \frac{r_{tc}^2}{r_{jc}^2} \frac{d}{d\phi} \tau_t(\phi) + \frac{C_{w1}(\phi)}{r_{jc}} \quad (j = t, b), \end{aligned} \tag{20}$$

where $C_{w1}(\phi)$ is a coefficient of integration to be determined through the compatibility conditions (8) at the face-core interfaces; $\tau_j(\phi)$ and $\sigma_{rrj}(\phi)$ ($j = t, b$) are the shear and radial normal stresses, respectively,

at the face-core interfaces. The result for the radial stress field is

$$\sigma_{rr}(\phi, r_c) = \frac{cE_{rc}\alpha_{Tc}}{2r_cL}(T_{ct}(\phi) + T_{cb}(\phi)) - \frac{E_{rc}}{r_cL}(w_t(\phi) - w_b(\phi)) + \left(\frac{r_{tc}c}{r_cr_{bc}L} + \frac{r_{tc}^2}{r_c^2}\right)\frac{d\tau_t(\phi)}{d\phi}, \quad (21)$$

where we have introduced the temperature functions T_{ct} and T_{bt} at the core-face interfaces, as well as the abbreviation

$$L = \ln \frac{r_{bc}}{r_{tc}}.$$

Equation (21) specializes to the vertical normal stresses at the upper and the lower face-core interfaces:

$$\begin{aligned} \sigma_{rrt}(\phi) &= \frac{cE_{rc}\alpha_{Tc}}{2r_{tc}L}(T_{ct}(\phi) + T_{cb}(\phi)) - \frac{E_{rc}}{r_{tc}L}(w_t(\phi) - w_b(\phi)) + \left(\frac{c}{r_{bc}L} + 1\right)\frac{d\tau_t(\phi)}{d\phi}, \\ \sigma_{rrb}(\phi) &= \frac{cE_{rc}\alpha_{Tc}}{2r_{bc}L}(T_{ct}(\phi) + T_{cb}(\phi)) - \frac{E_{rc}}{r_{bc}L}(w_t(\phi) - w_b(\phi)) + \left(\frac{r_{tc}c}{r_{bc}^2L} + \frac{r_{tc}^2}{r_{bc}^2}\right)\frac{d\tau_t(\phi)}{d\phi}. \end{aligned} \quad (22)$$

The displacement fields of the core in the radial and circumferential directions are determined through the constitutive relations (19) and the three compatibility conditions (8) at the upper face-core interface and the radial compatibility condition at the lower interface. They read as follows:

$$\begin{aligned} w_c(\phi, r_c) &= -\frac{\alpha_{Tc}}{2cL}\left((r_{tc} - r_c)^2L - c^2 \ln \frac{r_c}{r_{tc}}\right)T_{ct}(\phi) \\ &\quad + \frac{\alpha_{Tc}}{2cL}\left((r_{bc} - r_c)^2L + c^2 \ln \frac{r_c}{r_{bc}}\right)T_{cb}(\phi) \\ &\quad + \frac{1}{L}\left(w_b(\phi) \ln \frac{r_c}{r_{tc}} - w_t(\phi) \ln \frac{r_c}{r_{bc}}\right) \\ &\quad + \frac{r_{tc}}{E_cr_{bc}r_cL}\left(r_{tc}r_c \ln \frac{r_c}{r_{tc}} - r_{bc}r_c \ln \frac{r_c}{r_{bc}} - r_{tc}r_{bc}L\right)\frac{d\tau_t(\phi)}{d\phi} \end{aligned} \quad (23)$$

$$\begin{aligned} u_c(\phi, r_c) &= -\frac{\alpha_{Tc}}{2r_{tc}cL}\left(Lr_{tc}\left(r_c^2 - r_{tc}^2 - 2r_cr_{bc} \ln \frac{r_c}{r_{tc}} + 2c(r_{tc} - r_c)\right) - c^2\left(r_{tc}\left(1 + \ln \frac{r_c}{r_{tc}}\right) - r_c\right)\right)\frac{dT_{ct}(\phi)}{d\phi} \\ &\quad + \frac{\alpha_{Tc}}{2r_{tc}cL}\left(Lr_{tc}\left(r_c^2 - r_{tc}^2 - 2r_cr_{tc} \ln \frac{r_c}{r_{tc}}\right) + c^2\left(r_{tc} - r_c + r_{tc} \ln \frac{r_c}{r_{tc}}\right)\right)\frac{dT_{cb}(\phi)}{d\phi} \\ &\quad - \frac{1}{r_{tc}L}\left(r_{tc} - r_c + r_{tc} \ln \frac{r_c}{r_{bc}} + r_cL \frac{r_{tc}}{r_t}\right)\frac{dw_t(\phi)}{d\phi} \\ &\quad + \frac{1}{r_{tc}L}\left(r_{tc} - r_c + r_{tc} \ln \frac{r_c}{r_{tc}}\right)\frac{dw_b(\phi)}{d\phi} + \frac{r_c^2 - r_{tc}^2}{2r_cG_c}\tau_t(\phi) + \frac{r_c}{r_t}u_{ot}(\phi) \\ &\quad + \frac{1}{2E_cLr_{bc}r_c}\left(2cr_c(r_{tc} - r_c + r_{tc} \ln \frac{r_c}{r_{bc}}) + (2r_{tc}^2r_c - (r_{tc}^2 + r_c^2)r_{bc})L\right)\frac{d^2\tau_t(\phi)}{d\phi^2} \end{aligned} \quad (24)$$

Next we give the fifth of the field equations, which results from the compatibility condition at the lower face-core interface in the circumferential direction, and it derived using (8) and (24) along with a

nonuniform temperature field:

$$\begin{aligned} & \frac{\alpha_{Tc}}{2cr_{tc}L} (c^3 + 2r_{bc}r_{tc}L(c + r_{bc}L)) \frac{dT_{ct}(\phi)}{d\phi} + \frac{\alpha_{Tc}}{2cr_{tc}L} (c^3 - 2r_{bc}r_{tc}L(c + r_{tc}L)) \frac{dT_{cb}(\phi)}{d\phi} \\ & + \frac{r_{bc}}{r_t} u_{ot}(\phi) - \frac{r_{bc}}{r_b} u_{ob}(\phi) + \frac{2c^2 + (r_{tc}^2 - r_{bc}^2)L}{2E_{rc}r_{bc}L} \frac{d^2\tau_t(\phi)}{d\phi^2} - \frac{r_{tc}^2 - r_{bc}^2}{2r_{bc}G_{src}} \tau_t(\phi) \\ & + \left(\frac{c}{r_{tc}L} + \frac{r_{bc}}{r_b} \right) \frac{dw_b(\phi)}{d\phi} - \left(\frac{c}{r_{tc}L} + \frac{r_{bc}}{r_t} \right) \frac{dw_t(\phi)}{d\phi} = 0. \end{aligned} \quad (25)$$

However, when the temperature distribution is uniform through the length of the panel and the elastic constants are uniform, nothing is left of the first line and the compatibility equation becomes identical to the one obtained for the linear case [Frostig 1999]:

$$\begin{aligned} & \frac{r_{bc}}{r_t} u_{ot}(\phi) - \frac{r_{bc}}{r_b} u_{ob}(\phi) + \frac{2c^2 + (r_{tc}^2 - r_{bc}^2)L}{2E_{rc}r_{bc}L} \frac{d^2\tau_t(\phi)}{d\phi^2} - \frac{r_{tc}^2 - r_{bc}^2}{2r_{bc}G_{src}} \tau_t(\phi) \\ & + \left(\frac{c}{r_{tc}L} + \frac{r_{bc}}{r_b} \right) \frac{dw_b(\phi)}{d\phi} - \left(\frac{c}{r_{tc}L} + \frac{r_{bc}}{r_t} \right) \frac{dw_t(\phi)}{d\phi} = 0. \end{aligned} \quad (26)$$

The boundary condition of the core when an edge beam is attached to the end of the panel—see Equation (23)—and the global displacements,

$$w_{ge}(\phi_e) = w_t(\phi_e) = w_b(\phi_e) = 0,$$

require the use of the relaxed condition (18) within the core, which yields

$$\begin{aligned} & \frac{r_{tc}}{E_c r_{bc} L} (-c^2 + r_{bc} r_{tc} L^2) D(\tau_t)(\phi_e) \\ & - \frac{\alpha_{Tc} c}{6L} \left((3c + (3r_{tc} - c)L) T_{ct}(\phi_e) + (3c + (3r_{bc} + c)L) T_{cb}(\phi_e) \right) = 0. \end{aligned} \quad (27)$$

When the temperatures or coefficient of thermal expansion of the core is zero this condition yields $D(\tau_t)(\phi_e) = 0$ for the slope of the stress, which coincides with the linear case of [Frostig 1999].

Governing equations: uniform core (TI). The governing equations assume that the face sheets are isotropic. They are defined using the following load-displacement relations ($j = t, b$):

$$\begin{aligned} N_{ssj}(\phi) &= EA_j \left(\frac{1}{r_j} \left(\frac{du_{oj}(\phi)}{d\phi} + w_j(\phi) \right) + \frac{1}{2r_j^2} \left(u_{oj}(\phi) - \frac{dw_j(\phi)}{d\phi} \right)^2 - \frac{\alpha_{Tj}}{2} (T_{jt}(\phi) + T_{jb}(\phi)) \right), \\ M_{ssj}(\phi) &= EI_j \left(\frac{1}{r_j^2} \left(\frac{du_{oj}(\phi)}{d\phi} - \frac{d^2w_j(\phi)}{d\phi^2} \right) - \frac{\alpha_{Tj}}{d_j} (T_{jt}(\phi) - T_{jb}(\phi)) \right). \end{aligned} \quad (28)$$

The governing equations are derived upon substitution of these relations and the shear and radial normal stresses of the core at the upper and lower interfaces, namely (20) and (22), into the equilibrium

equations (9)–(10). This gives

$$\begin{aligned} \frac{1}{r_t} \left(u_{ot}(\phi) - \frac{dw_t(\phi)}{d\phi} \right) N_{sst}(\phi) + \frac{b_w r_{tc}^2}{r_t} \tau_t(\phi) - r_t n_t + m_t(\phi) - \frac{1}{r_t} \frac{dM_{sst}(\phi)}{d\phi} - \frac{dN_{sst}(\phi)}{d\phi} &= 0, \\ \frac{1}{r_b} \left(u_{ob}(\phi) - \frac{dw_b(\phi)}{d\phi} \right) N_{ssb}(\phi) - \frac{b_w r_{bc}^2}{r_b} \tau_t(\phi) - r_b n_b + m_b(\phi) - \frac{1}{r_b} \frac{dM_{ssb}(\phi)}{d\phi} - \frac{dN_{ssb}(\phi)}{d\phi} &= 0, \\ \frac{b_w E_{rc}}{L} (w_b(\phi) - w_t(\phi)) + \frac{\alpha_{Tc} b_w c E_{rc}}{2L} (T_{ct}(\phi) + T_{cb}(\phi)) \\ + b_w r_{tc} \left(\frac{r_{tc}}{r_t} + \frac{c}{r_{bc} L} \right) \frac{d\tau_t(\phi)}{d\phi} + \frac{1}{r_t} \left(u_{ot}(\phi) - \frac{dw_t(\phi)}{d\phi} \right) \frac{dN_{sst}(\phi)}{d\phi} \\ + \left(1 + \frac{1}{r_t} \left(\frac{du_{ot}(\phi)}{d\phi} - \frac{d^2 w_t(\phi)}{d\phi^2} \right) \right) N_{sst}(\phi) - r_t q_t + \frac{d}{d\phi} m_t(\phi) - \frac{1}{r_t} \frac{d^2 M_{sst}(\phi)}{d\phi^2} &= 0, \\ \frac{b_w E_{rc}}{L} (w_t(\phi) - w_b(\phi)) - \frac{\alpha_{Tc} b_w c E_{rc}}{2L} (T_{ct}(\phi) + T_{cb}(\phi)) \\ - b_w r_{tc} \left(\frac{r_{tc}}{r_b} + \frac{c}{r_{bc} L} \right) \frac{d\tau_t(\phi)}{d\phi} + \frac{1}{r_b} \left(u_{ob}(\phi) - \frac{dw_b(\phi)}{d\phi} \right) \frac{dN_{ssb}(\phi)}{d\phi} \\ + \left(1 + \frac{1}{r_b} \left(\frac{du_{ob}(\phi)}{d\phi} - \frac{d^2 w_b(\phi)}{d\phi^2} \right) \right) N_{ssb}(\phi) - r_b q_b + \frac{d}{d\phi} m_b(\phi) - \frac{1}{r_b} \frac{d^2 M_{ssb}(\phi)}{d\phi^2} &= 0. \end{aligned}$$

To these four equilibrium equations one must add (25) to obtain the full set of governing equations.

4. Temperature dependence: general solution for the core stress and displacement fields

We now take into account the possibility that the mechanical core properties vary with the radial coordinate, as they must if these properties are temperature-dependent and there is a temperature gradient. Specifically, we determine the general solution for the stress and displacement fields within the depth of the core for an isotropic core with the constitutive relations (19), which we copy here adding an explicit dependence of the Young's and shear moduli of the core (E_{rc} and G_{src}) on the radial coordinate r_c :

$$\begin{aligned} \varepsilon_{rr}(\phi, r_c) &= \frac{\sigma_{rr}(\phi, r_c)}{E_{rc}(r_c)} + \alpha_{Tc} T_c(r_c, \phi), \\ \gamma_{sr}(\phi, r_c) &= \frac{\tau_{sr}(\phi, r_c)}{G_{src}(r_c)}, \end{aligned} \tag{29}$$

The displacement fields are derived using these constitutive relations, the expressions (20) for the stress fields, the kinematic relations (7), the compatibility conditions (8) at the upper face-core interface (that is, with $j = t$), and the compatibility condition (8)₂ in the vertical direction at the lower face-core interface ($j = b$). Hence, the general expression of these fields with the constants of integration where

the temperature distribution through the depth of the core is linear (Figure 1) is

$$w_c(\phi, r_c) = \frac{\alpha_{Tc} r_c}{2c} ((r_c - 2r_{bc})T_{ct}(\phi) - (r_c - 2r_{tc})T_{cb}(\phi)) + \frac{d\tau_t(\phi)}{d\phi} r_{tc}^2 \int \frac{1}{r_c^2 E_{rc}(r_c)} dr_c + C_{w1}(\phi) \int \frac{1}{r_c E_{rc}(r_c)} dr_c + C_{w2}(\phi), \quad (30)$$

$$u_c(r_c, \phi) = \frac{\alpha_{Tc} r_c}{2c} \left((2r_{bc} \ln(r_c) - r_c) \frac{dT_{ct}(\phi)}{d\phi} - (2r_{tc} \ln(r_c) - r_c) \frac{dT_{cb}(\phi)}{d\phi} \right) + \frac{dC_{w2}(\phi)}{d\phi} + r_c C_u(\phi) - r_c r_{tc}^2 \frac{d^2 \tau_t(\phi)}{d\phi^2} \int \int \frac{1}{r_c^2 E_{rc}(r_c)} dr_c - r_c \frac{dC_{w1}(\phi)}{d\phi} \int \int \frac{1}{r_c E_{rc}(r_c)} dr_c + r_c \tau_t(\phi) r_{tc}^2 \int \frac{1}{G_{src}(r_c) r_c^3} dr_c, \quad (31)$$

where $\tau_t(\phi)$ is the shear stress at the upper face-core interface and is used as an unknown, similar to the shear stress unknown in the HSAPT model; C_{w_j} ($i = 1, 2$) are the constants of integration to be determined through the compatibility conditions (8) imposed in the radial directions; and C_u is a constant of integration to be determined by the compatibility requirement (8)₁ for the circumferential displacement at the upper face-core interface.

Nonuniform core moduli. A core with nonuniform mechanical properties occurs when the properties are temperature-dependent (TD), or when it is made of a functionally graded material. In such a case the stress and displacement fields may be determined analytically only when the distribution of the moduli is of the fourth order. However, in order to achieve a general closed-form description of the core fields we describe the moduli, or more precisely their inverses, by a polynomial series:

$$E_{rc}(r_c) = \frac{1}{\sum_{i=0}^{N_e} E_i r_c^i}, \quad G_{src}(r_c) = \frac{1}{\sum_{i=0}^{N_e} G_i r_c^i}, \quad (32)$$

where E_i and G_i are the coefficients of the polynomial description of the elastic moduli functions, and N_e is the number of terms in the polynomial. This polynomial description can be determined through curve fitting procedures or Taylor series. The number of terms depends on the required accuracy to describe of the inverse moduli.

The displacement field of the core is derived through the substitution of the moduli functions (32) into (30) and (31), which yields

$$w_c(\phi, r_c) = r_{tc}^2 \left(-\frac{E_0}{r_c} + E_1 \ln(r_c) + E_2 r_c + \sum_{i=3}^{N_e} \frac{E_i r_c^{i-1}}{i-1} \right) \frac{d\tau_t(\phi)}{d\phi} + \left(E_0 \ln(r_c) + E_1 r_c + \frac{E_2}{2} r_c^2 + \sum_{i=3}^{N_e} \frac{E_i r_c^i}{i} \right) C_{w1}(\phi) + \frac{r_c}{2c} ((r_c - 2r_{bc})T_{ct}(\phi) + (-r_c + 2r_{tc})T_{cb}(\phi)) \alpha_{Tc} + C_{w2}(\phi), \quad (33)$$

$$\begin{aligned}
u_c(\phi, r_c) = & r_{ic}^2 r_c \left(-\frac{E_0}{2r_c^2} + \frac{E_1}{r_c} (\ln(r_c) + 1) - E_2 \ln(r_c) - \sum_{i=3}^{N_e} \frac{E_i r_c^{i-2}}{(i-1)(i-2)} \right) \frac{d^2 \tau_t(\phi)}{d\phi^2} \\
& + r_c \left(\frac{E_0}{r_c} (\ln(r_c) + 1) - E_1 \ln(r_c) - \frac{E_2}{2} r_c - \sum_{i=3}^{N_e} \frac{r_c^{i-1} E_i}{(i-1)i} \right) \frac{dC_{w1}(\phi)}{d\phi} \\
& + \frac{\alpha_{Tc} r_c}{2c} \left((2r_{bc} \ln(r_c) - r_c) \frac{dT_{ct}(\phi)}{d\phi} - (2r_{ic} \ln(r_c) - r_c) \frac{dT_{cb}(\phi)}{d\phi} \right) \\
& + r_{ic}^2 r_c \left(-\frac{G_0}{2r_c^2} + G_2 \ln(r_c) - \frac{G_1}{r_c} + G_3 r_c + \sum_{i=4}^{N_e} \frac{G_i r_c^{i-2}}{i-2} \right) \tau_t(\phi) + \frac{d}{d\phi} C_{w2}(\phi) + r_c C_u(\phi). \quad (34)
\end{aligned}$$

Note that the first three or four terms in the polynomial description are not within the sum terms since they involve integration of $1/r_c$ terms.

The constants of integrations C_{w1} and C_{w2} are determined by applying the compatibility conditions (8)₂ in the vertical direction to the vertical displacement (33) of the core. The third constant of integration, C_u , is determined by imposing the compatibility condition (8)₁ at the upper face-core interface on the displacement (34) in the circumferential direction. The vertical normal stresses within the core and are determined by substitution of the vertical constant of integration in the vertical normal stress distribution, see (20). The fifth governing equation, denoted also as the compatibility equation, which imposes the compatibility condition (8)₁ in the circumferential (in-plane) direction at the lower face-core interface, is determined through substitution of the three constants of integration into the expression (34) for the circumferential displacements of the core. The explicit description of the stress and displacement fields is very lengthy and is not presented herein for brevity.

5. Numerical study

The numerical solution of the nonlinear differential equations can be achieved using numerical schemes such as the multiple-shooting points method [Stoer and Bulirsch 1980] or the finite-difference (FD) approach using trapezoid or mid-point methods with Richardson extrapolation or deferred corrections [Ascher and Petzold 1998], as implemented in Maple, along with parametric or arc-length continuation methods [Keller 1992]. The FD approach as implemented in Maple has been used in this study. It is robust and includes error control along with an arc-length procedure built-in. These solution approaches have been used by the authors in many cases and have been compared also recently with FE nonlinear codes; see for example [Frostig and Thomsen 2008b].

We studied the thermomechanical nonlinear response of a simply supported and clamped shallow curved sandwich panel subjected to a concentrated and distributed load, as shown in Figure 4. The sandwich panel consists of two aluminum face sheets of a thickness of 1 mm and an H60 PVC foam core made by Devinicell with $E_c = 56.7$ MPa and $G_c = 22$ MPa and with a thickness of 25 mm. The geometry of the curved panel is that of an experimental set-up used in [Bozhevolnaya and Frostig 1997; Bozhevolnaya 1998]; see Figure 4. The edges of the curved sandwich panel are reinforced by an edge beam and assumed to be bonded to the adjacent core (Detail A in the figure). The supporting system

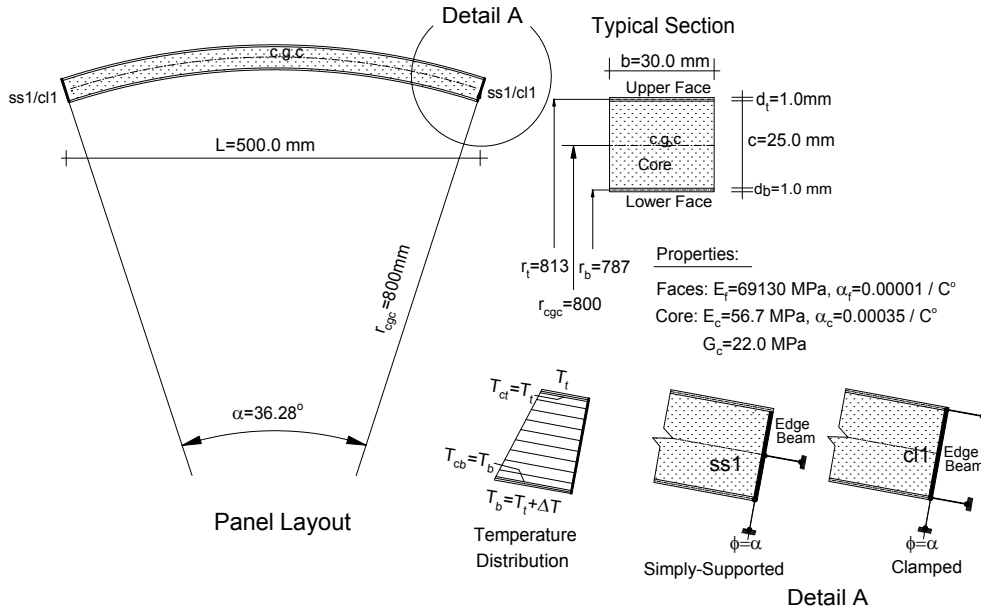


Figure 4. Geometry, dimensions, mechanical properties, temperature distribution and supporting systems of the shallow curved panel under investigation.

prevents circumferential displacement in addition to the other constraints. The simply supporting system is denoted by ss1 and the clamped one by cl1.

Under the assumption of TI core properties, the mechanical response of the curved sandwich panel subjected to a concentrated load at mid-span and a distributed load, and without the response induced by thermal loading, is described first. This is followed by a description of the thermal response without the mechanical loads, and a presentation of the case of simultaneous mechanical and thermal loading.

Finally the effects of the thermal degradation of the core properties with elevated temperature (TD setting) are studied first for thermal loading only, then for combined thermal and mechanical loading.

A symmetric analysis has been considered using symmetry conditions at mid-span.

5.1. Temperature-independent mechanical properties.

Mechanical loading only. The nonlinear mechanical response of a sandwich panel when subjected to a concentrated load that is applied at mid-span to the upper face sheet appears in Figures 5 and 6, with two types of supporting systems. The results include the deformed shape and equilibrium curves of load versus extreme values of selected structural quantities.

The deformed shapes of a simply supported curved sandwich panel appear in Figure 5, left, from which is it seen that prior to the limit point, indicated in Figure 6(a), the panel exhibits indentation at the upper face sheet, which becomes significant as the mid-span displacement increases. In the clamped case, shown in Figure 5, right, the same trends at mid-span as for the first supporting system are observed, while in the vicinity of the clamped support local buckling occurs for large mid-span displacements far beyond the limit point.

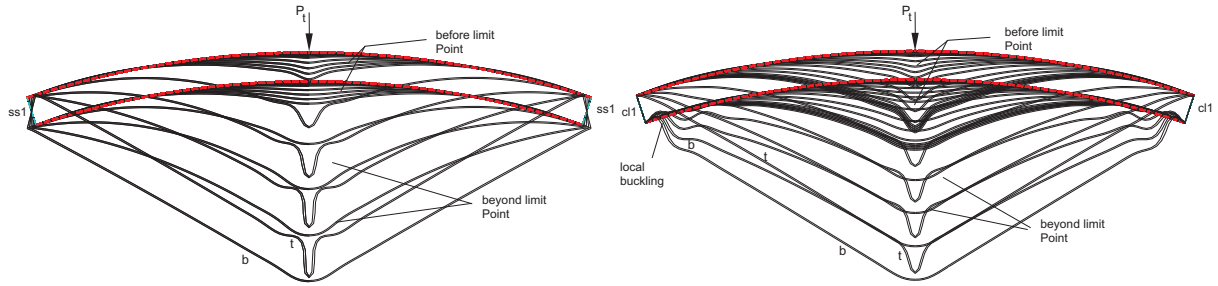


Figure 5. Deformed shapes of the curved panel when loaded by a *concentrated mechanical load* for the two supporting systems. Left: simply supported; right: clamped.

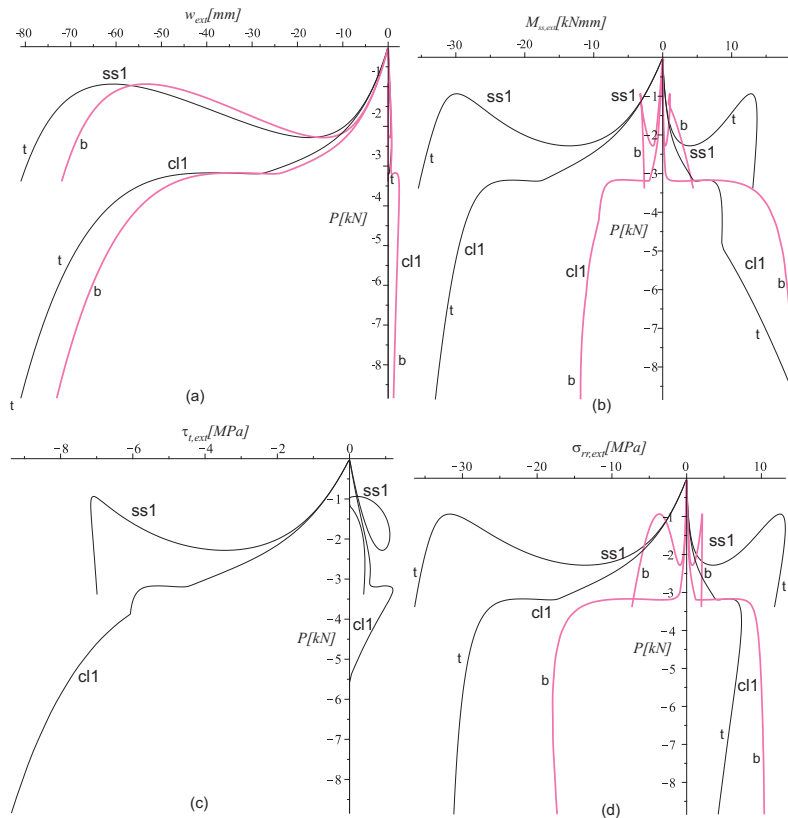


Figure 6. Equilibrium curves of load versus extreme values of (a) vertical displacements of face sheets, (b) bending moments in faces, (c) shear stress in core, and (d) interfacial radial normal stresses at face-core interfaces, all for curved sandwich panel subjected to *concentrated mechanical loading* at mid-span of upper face sheet. Thin black lines (marked t) refer to the upper face sheet; thicker pink lines (marked b) to the lower one.

The equilibrium curves of load versus extreme values of structural quantities of the two supporting systems appear in Figure 6. In part (a) we see the load versus the extreme vertical displacement along the sandwich panel. It reveals that the nonlinear response is characterized by a limit point behavior for

both supporting systems. The limit point load for the simply supporting system is lower than that of the clamped case, and it occurs also at a lower displacement as compared with the clamped case. In the *ss1* case there is a decrease in the vertical displacement beyond the limit point value which changes into an increasing branch as the displacement reaches larger values. The trends are different in the clamped case, and they consist of a plateau beyond the limit point displacement followed by an increasing branch. The trends are similar for the upper and lower faces. The plot of load versus extreme bending moments in the face sheets, shown in Figure 6(b), exhibits similar trends for the upper face sheet (thin black curves marked “t”) but quite erratic behavior for the lower one (thicker pink curves marked “b”). Notice that the curves describe the *extreme* values for each load level which do not necessarily occur at the same section. The interfacial shear stresses at the upper face-core interface appear on Figure 6(c), and they exhibit a limit point behavior but with a reduction in their values on the increasing branch for the simply supporting case and an increase for the clamped case. The interfacial radial normal stresses at the upper and lower face-core interfaces appear in Figure 6(d), which reveals trends similar to those observed for the vertical displacements.

The nonlinear mechanical response of the curved sandwich panel due to a fully distributed load exerted at the upper face sheet appears in Figure 7 and 8. The deformed shapes here reveal that at the limit point and beyond it a nonsinusoidal localized local buckling of the mid-span of the upper face sheet occurs. In the clamped case, there is an additional local buckling in the vicinity of the support at the lower face sheet similar to the case with the concentrated load.

The equilibrium curves for this loading scheme appears in Figure 8. The curves of distributed load versus extreme vertical displacement of the face sheets, shown in part (a), reveal a limit point behavior for both supporting systems, where the load at the limit point of the clamped case is a little bit larger than that of the simply supported case, and occurring at similar displacements values. In both cases a very steep descending branch is observed beyond the limit point. The bending moment curves, shown in part (b), exhibit similar trends but with very steep slopes of branches prior to and beyond the limit point. The plot versus upper interfacial shear stresses, in Figure 8(c), exhibits a limit point behavior similar to that of the vertical displacements. The interfacial normal stress curves follow the trends of the bending moments diagram with an abrupt change at the limit point. At the end of the descending branch of the simply supported case the interfacial shear and vertical normal stresses at the upper face-core interface decrease as the vertical displacements increase, as seen in parts (c) and (d) of the figure. Note also that the differences between the simply supporting and the clamped cases are minor.

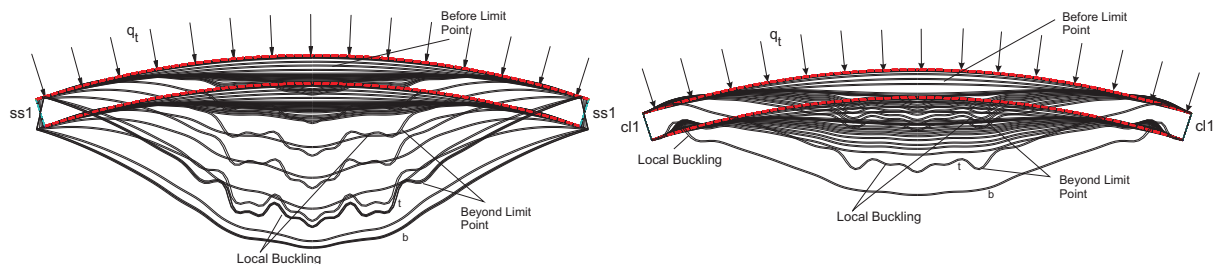


Figure 7. Deformed shapes of the curved panel when loaded by a fully *distributed mechanical load* for the two supporting systems. Left: simply supported; right: clamped.

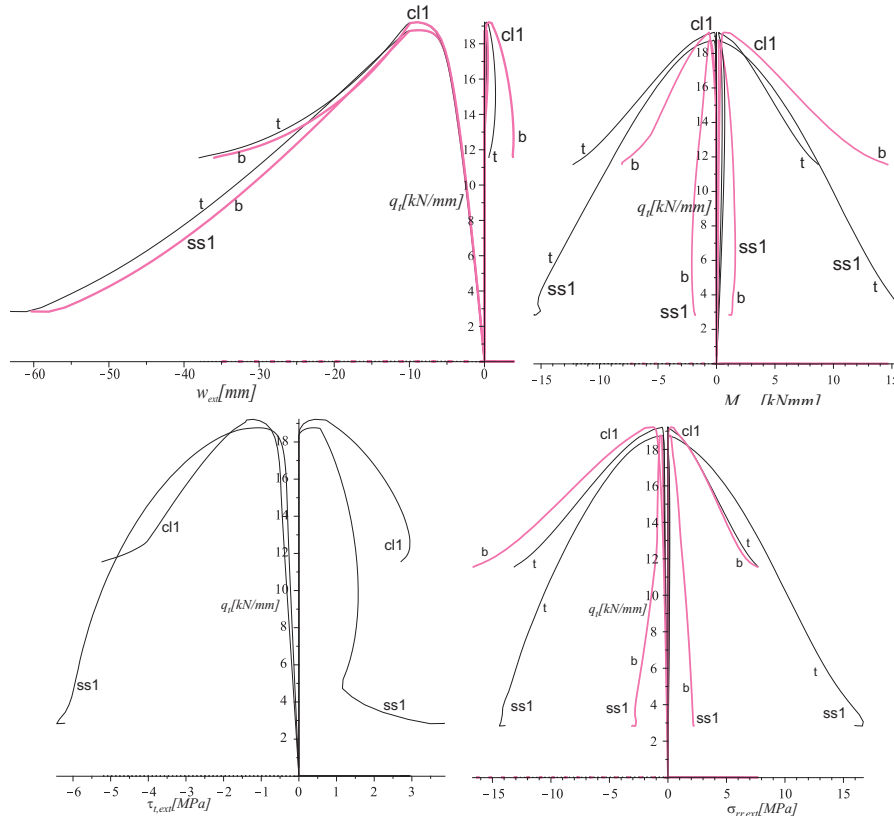


Figure 8. Equilibrium curves of load versus extreme values of (a) vertical displacements of face sheets, (b) bending moments in faces, (c) shear stress in core, and (d) interfacial radial normal stresses at face-core interfaces, all for curved sandwich panel subjected to a *distributed mechanical load* only, applied at the upper face sheet. Thin black lines (marked t) refer to the upper face sheet; thicker pink lines (marked b) to the lower one.

Thermal loading only. The thermal response of a curved sandwich panel subjected to a uniformly distributed temperature through its length and thickness is displayed in Figures 9 and 10. This response is linear throughout the range of temperatures investigated. The deformed shapes for temperatures from 0 to 200°C (heating) appear on the left in Figure 9, and those for temperatures from 0 to -200°C (cooling) on the right. In the case of heating, the two faces move upwards around mid-span while in the vicinity of the supports the expansion of the core involves localized changes in the curvature of the two face sheets. By contrast, under cooling the two face sheets move downwards around mid-span while near the



Figure 9. Deformed shapes of the curved sandwich panel subjected to *thermal loading* (left: heating; right: cooling) with no mechanical load.

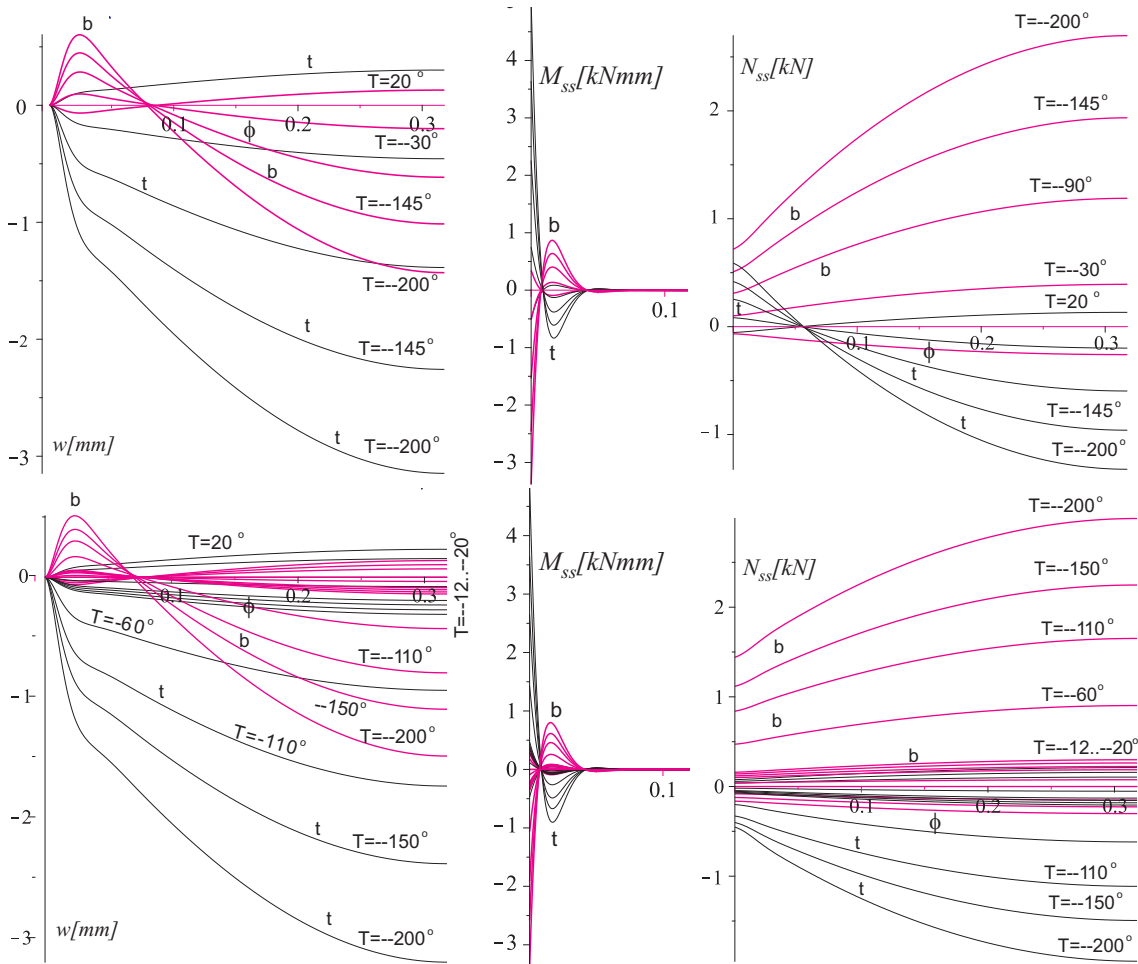


Figure 10. Cooling *thermal loading* results for face sheets along the panel circumference for simply supported (top) and clamped (bottom) systems. The horizontal coordinate is ϕ in all cases; all temperatures in degrees Celsius. Left column: vertical displacements. Middle column: bending moments. Right column: In-plane stress resultant (in core). Thinner black lines marked “t” stand for the upper face or interface; thicker, pink lines marked “b”, for the lower.

supports the core contracts, along with localized bending moments in the face sheets. Notice also that the pattern of displacements is in the opposite direction to that of the external loads (Figures 5 and 7) when heating is considered.

The vertical displacements, the bending moments and the circumferential stress resultants in the faces, along half of the sandwich panel, for the two supporting systems under a cooling temperature pattern appear in Figure 10. The displacement curves for the various temperatures (left column) and the bending moment diagrams (middle column) are almost the same for the two supporting systems. Notice that bending moments occur only in the vicinity of the supports, as a result of the contraction of the core that causes changes in the curvatures of the face sheets. The circumferential forces (normal stress resultants)

in the face sheets (rightmost column of Figure 10) reveal that in the case of a simply supported panel the stress resultants at the edges in the two face sheets are in tension, and around mid-span the upper face sheet is in compression whereas the lower face sheet is in tension. In the case of a clamped support the circumferential stress resultants differs from that of the simply supported case, and the resultants in the upper face sheets are in compression while those of the lower face are in tension. It should be noticed that in the case of elevated temperatures the displacements and the stress resultant patterns in the face sheets and the core are opposite to those observed for the cooling case, which yields that the upper face sheets is in tension while the lower one is in compression. Thus, the heating temperature pattern yields stress resultants that cancel out the stress resultants of the external mechanical loads that appear in Figures 5 and 7. The response is similar when the temperature distribution has a gradient between the two face sheets.

Thermomechanical loading. The thermomechanical response of the curved sandwich panel subjected to a concentrated load applied at mid-span of the upper face sheet along with a circumferentially uniform temperature with a gradient of 40°C between the upper and lower face sheet is considered next; see Figure 11. The study reveals that the combined response is linear when the applied mechanical loads are up to 80% of the load at the limit point. The thermomechanical response when elevated temperatures are considered exhibits a linear behavior since the thermal and mechanical responses act in opposite directions.

A nonlinear thermomechanical response is observed only when cooling temperatures are considered, and the external loads are in the range of 80–90% of the limit point load levels, as shown in Figures 12 and 13. The equilibrium curve of temperature versus the extreme vertical displacement of the face sheets appear in Figure 12a. It reveals that a limit point behavior is observed at about -150°C , when a simply supported panel is considered while in the case of a clamped panel the response is linear within the range of temperatures considered. Note that there is an initial displacement due to the existence of the external load prior to the application of the thermal loading. The bending moment diagrams, the upper interfacial shear stress and the interfacial normal stresses at the two face sheets (Figures 12b, 12c and 12d) exhibit similar trends. Note that the larger vertical normal stresses are in compression (Figure 12d).

The deformed shapes of the combined response for the two supporting systems at different temperature levels appear in Figure 11. The deformed shapes reveal a large indentation at mid-span for both supporting systems which deepens beyond the limit point (Figure 11, left) for the simply supported case and remain linear for the clamped case. Note that the deformed shapes corresponding to the limit point resemble those of the concentrated load only, shown in Figure 5.

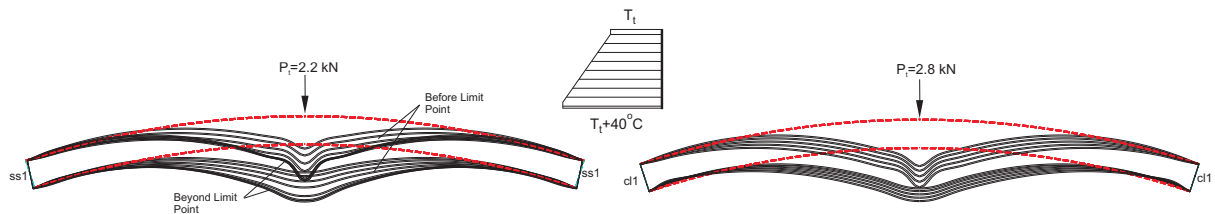


Figure 11. Deformed shapes of curved sandwich panel subjected simultaneously to a *concentrated mechanical load* and *thermal loading*. Left: simply supported; right: clamped.

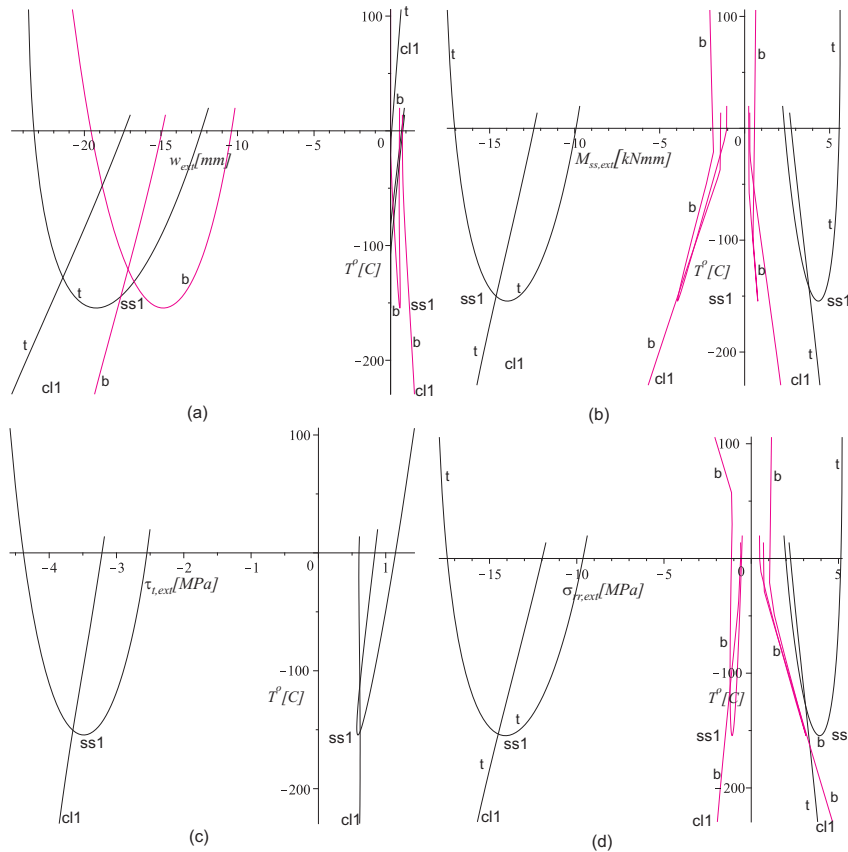


Figure 12. Equilibrium curves of load versus extreme values of (a) vertical displacements of faces sheets, (b) bending moments in faces, (c) shear stress in core, and (d) interfacial radial normal stresses at face-core interfaces, all for curved sandwich panel subjected to a *concentrated mechanical load* applied at mid-span of upper face sheet and *thermal loading* with a *temperature gradient* of 40°C at the lower face sheet. Thin black lines (marked t) refer to the upper face sheet; thicker pink lines (marked b) to the lower one.

The results along half the panel circumference of the combined thermomechanical response for a simply supported sandwich panel at different temperatures appear in Figure 13. The vertical displacements of the upper face sheets (Figure 13a) reveal a deepening indentation as the temperature level drops and the limit point is reached. It is observed that at temperatures above zero (before and beyond the limit point) the two face sheets move upwards in the vicinity of the support as a result of the core expansion, and the indentation disappears as the temperatures are lowered. Significant bending moments in the face sheets are observed in the vicinity of the external load and at the supports (Figure 13b). The magnitude increases as the temperatures are lowered and approach the limit point temperature level. The upper interfacial shear stress diagram reveals high values in the vicinity of the load and the support as well as shear stresses throughout the length of the panel (Figure 13c). The vertical interfacial stresses at both face sheets (Figure 13d), yield compressive as well as tensile stresses in the vicinity of the concentrated

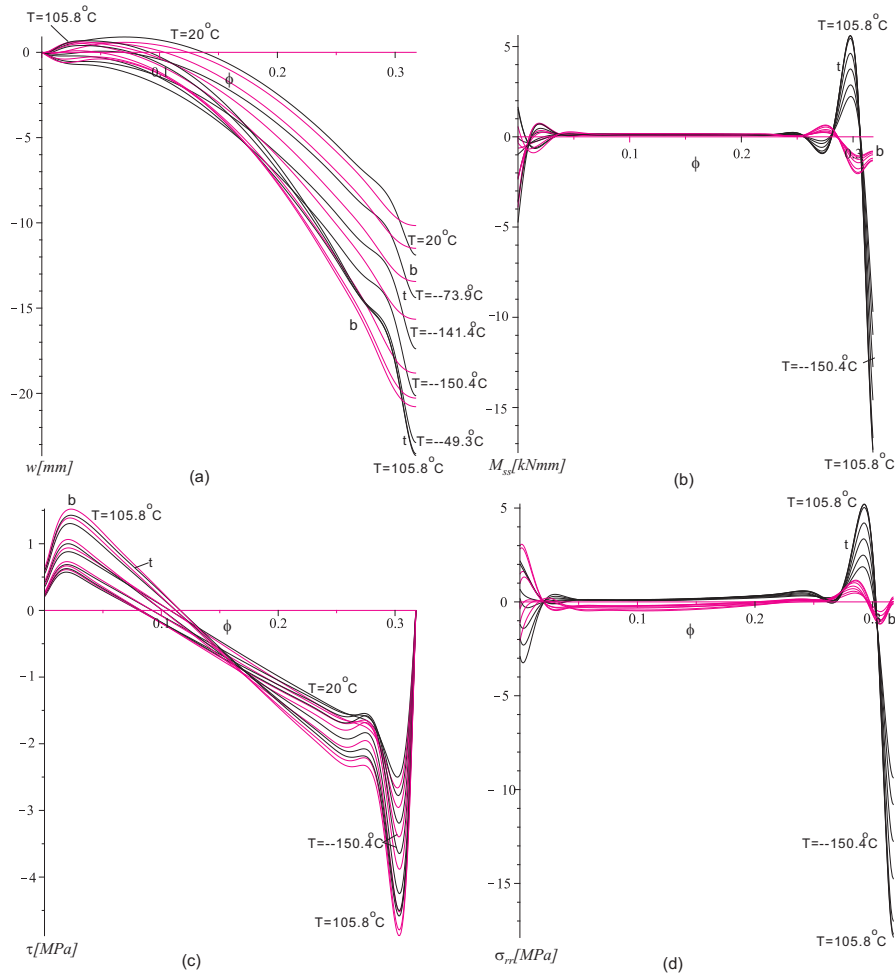


Figure 13. Thermomechanical response results for face sheets along the panel circumference for simply supported system when subjected to a *concentrated mechanical load* applied at mid-span of upper face sheet and *thermal loading* as in the previous figure. Shown are (a) vertical displacements, (b) bending moments, (c) shear stresses in face-core interfaces, and (d) radial normal stresses in same. Thinner black lines marked “t” stand for the upper face or interface; thicker, pink lines marked “b”, for the lower.

load that increase as the temperature approaches low levels. In addition, there is some accumulation of stresses in the vicinity of the support.

The combined thermomechanical response when a distributed load is applied at the upper face sheet and the temperature pattern is uniformly in the circumferential direction and with a gradient through the depth of the panel (Figure 14) is studied next. The combined response is linear as long as the distributed load is below 90% of the level corresponding to the limit point load as well as when the temperatures are above zero. The nonlinear response is presented in Figures 15 and 16 for a distributed load of a 1.7 kN/mm for the simply supported system and 1.741 kN/mm for the clamped case. For both supporting systems the distributed loads are applied at the upper face of the sandwich panel. Note that the applied

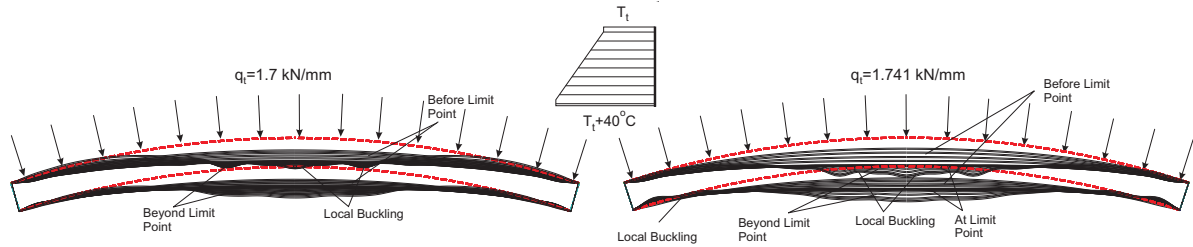


Figure 14. Deformed shapes of curved sandwich panel loaded simultaneously by a distributed load and thermal loading. Left: simply supported; right: clamped.

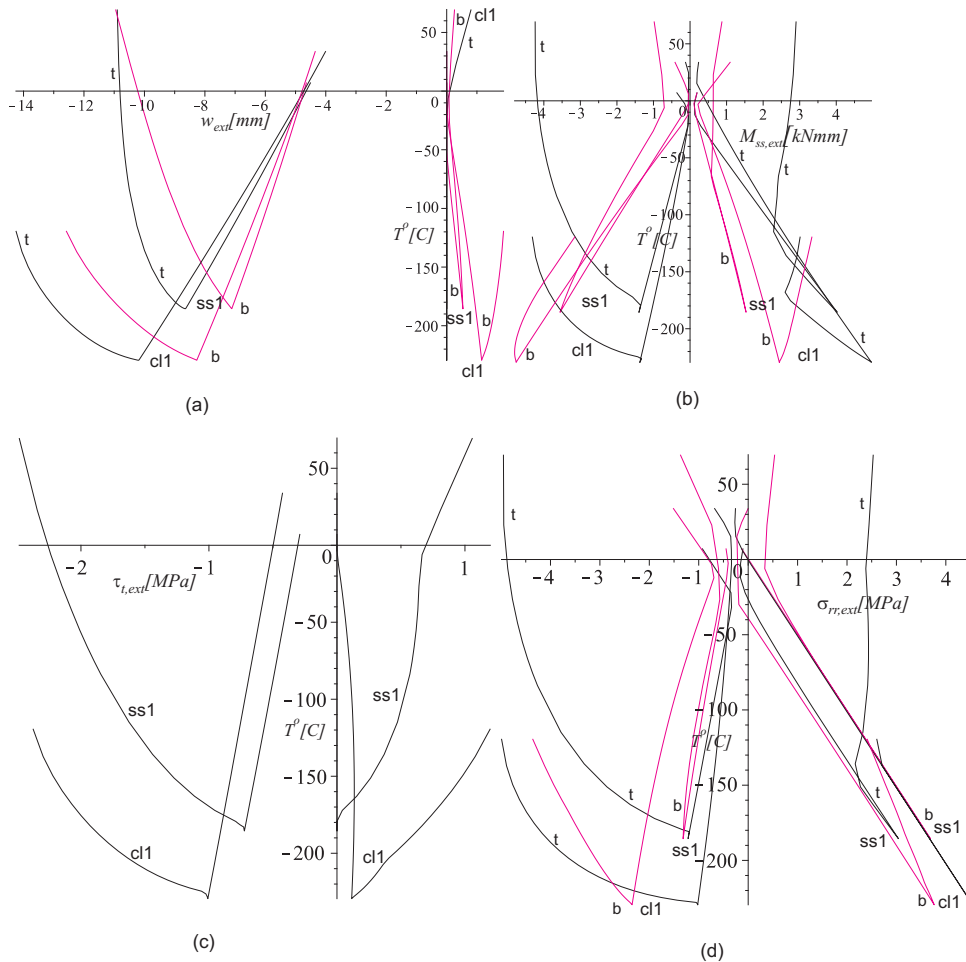


Figure 15. Equilibrium curves of load versus extreme values of (a) vertical displacements of faces sheets, (b) bending moments in faces, (c) shear stress in core, and (d) interfacial radial normal stresses at face-core interfaces, all for curved sandwich panel subjected to a **distributed mechanical load** to the upper face sheet and a **thermal loading** as in the previous figure. Thin black lines (marked t) refer to the upper face sheet; thicker pink lines (marked b) to the lower one.

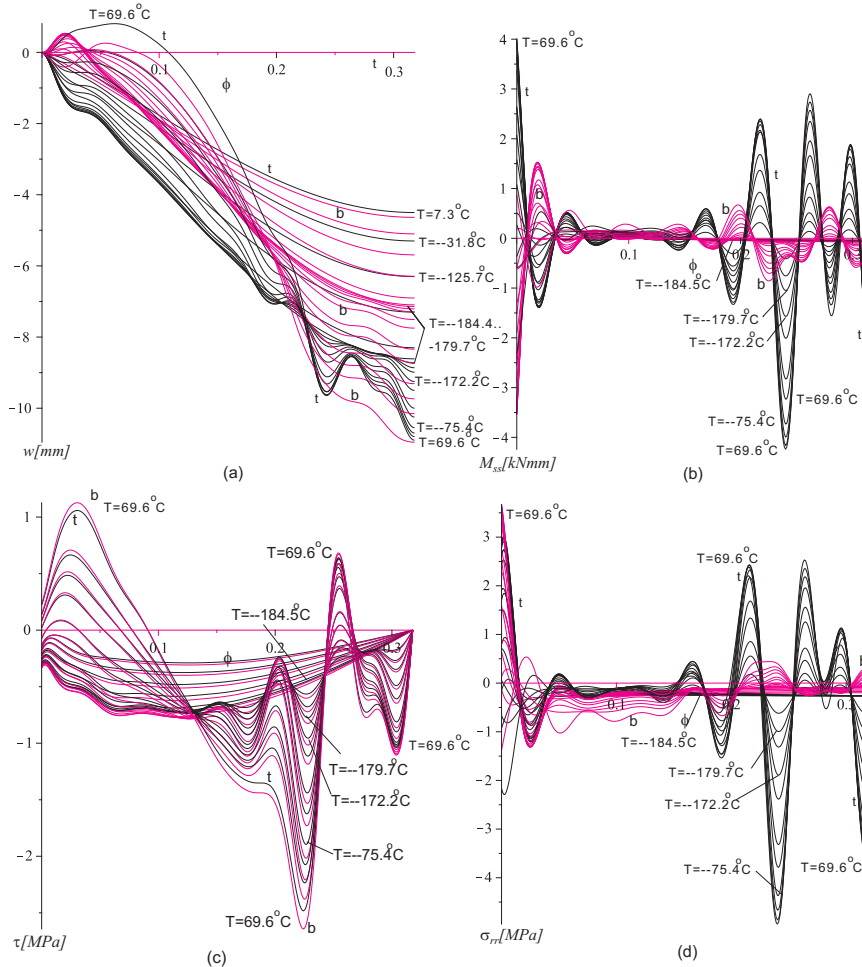


Figure 16. Thermomechanical response results for face sheets along the panel circumference for simply supported system when loaded by a *distributed mechanical load* on the upper face sheet and *thermal loading* as in the figures on the previous page. Shown are (a) vertical displacements, (b) bending moments, (c) shear stresses in face-core interfaces, and (d) radial normal stresses in same. Thinner black lines marked “t” stand for the upper face or interface; thicker, pink lines marked “b”, for the lower.

distributed loads represent 90.5% of the appropriate limit load level with no thermal loading; see Figure 8. For details see Figure 14.

The equilibrium curves of temperature versus extreme values of selected structural quantities reveal a limit point behavior for the two supporting systems with similar trends. The temperature versus the extreme vertical displacement of the face sheets (see Figure 15a) exhibits a limit point for both supporting systems. In the simply supported case the limit point occurs at -184.5°C , while in the clamped case the limit point is reached at a temperature of -229.47°C . In both cases the descending branches, prior to the limit point, are almost linear while the ascending branch, beyond the limit point, are nonlinear in general. The bending moment curves follow the same trends but with abrupt changes at the limit point

almost like that of a bifurcation behavior (Figure 15b). Note that the lower face sheet exhibits linear branches before and after the limit point, while the second branch, beyond the limit point descends. The upper interfacial shear stresses appear in Figure 15c and follow the trends of the bending moment curves. Similarly, the interfacial normal stresses exhibit a linear behavior prior to the limit point and a nonlinear one beyond that, following the trends of the bending moments.

The deformed shapes of the combined response for the two supporting systems appear in Figure 14. The two supporting systems exhibits a linear response up to the limit point and then they both yield a localized local buckling region around mid-span at temperatures in the vicinity of the limit point temperature level and beyond it. In addition local buckling of the lower face sheet occurs in the vicinity of the support in the case of a clamped panel. The characteristics of the deformed shape at the limit point and above resemble those found for the case of a distributed load and no thermal loading, shown in Figure 7.

The results along half of the panel circumference at different temperatures appear in Figure 16. The vertical displacements of the face sheets (Figure 16a) reveal that at the limit-point displacement local buckling waves appear which deepens on the ascending branch of the equilibrium curve (Figure 15a). This local buckling phenomenon is explicitly observed in the bending moment figure (Figure 16b) and the vertical normal interfacial stresses (Figure 16d). The local buckling affects also the interfacial shear stresses (Figure 16c). In general, the ripple characterization of the local buckling of the upper face sheet affects the response both globally and locally.

5.2. Temperature-dependent mechanical properties. This part of the investigation deals with the response of a curved sandwich panel subjected only to thermal loading, followed by a study of the same panel when subjected to combined thermal and mechanical loading. Both concentrated and distributed mechanical loads are considered, and again both simple support and clamped supporting systems are included in the study. The temperature-dependent core material properties adopted here follow those given by Burmann [2005a; 2005b] for cross-linked PVC Divinycell foams (from DIAB AB, Sweden) for a working range of temperatures between 20°C to 80°C.

The mechanical properties of the Divinycell foams degrade with increasing temperatures. For this study the temperature-dependent mechanical core material properties are defined through curve fitting of the data that appears in the manufacturer's data sheet [DIAB 2003] as follows:

$$E_c(\phi, r_c) = E_{co} f_T(T_c(\phi, r_c)), \quad G_c(\phi, r_c) = G_{co} f_T(T_c(\phi, r_c)),$$

where E_{co} and G_{co} refer to the Young's and shear moduli of the core at $T = 20^\circ\text{C}$, and

$$\begin{aligned} f_T(T) = & 1.1903 + 0.03070734934T - 0.009541812399T^2 + 0.0008705288588T^3 \\ & - 0.00003952259514T^4 + 9.70315767110^{-7}T^5 - 1.32513499810^{-8}T^6 \\ & + 9.52831997110^{-11}T^7 - 2.82196349610^{-13}T^8, \quad (35) \end{aligned}$$

where T is expressed in degrees Celsius. Note that when a thermal gradient is applied to the core the mechanical properties will also be dependent on the radial (through-the-thickness) coordinate. For more details see [Frostig and Thomsen 2008b]. In order to use the polynomial expansion (32) of the inverse of the moduli, the coefficients must be found using Taylor series or curve-fitting tools.

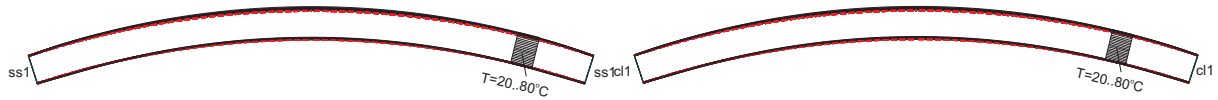


Figure 17. Deformed shapes of curved sandwich panel subjected to uniform *thermal loading* and with *temperature-dependent core properties*. Left: simply supported; right: clamped.

Thermal loading only. The deformed shapes of the curved sandwich panel subjected to thermal loading only appears in Figure 17, and the predicted response in Figures 18 and 19. Figure 17 shows that, for both supporting systems, the panel moves upward as the temperature is increased and the core properties degrade.

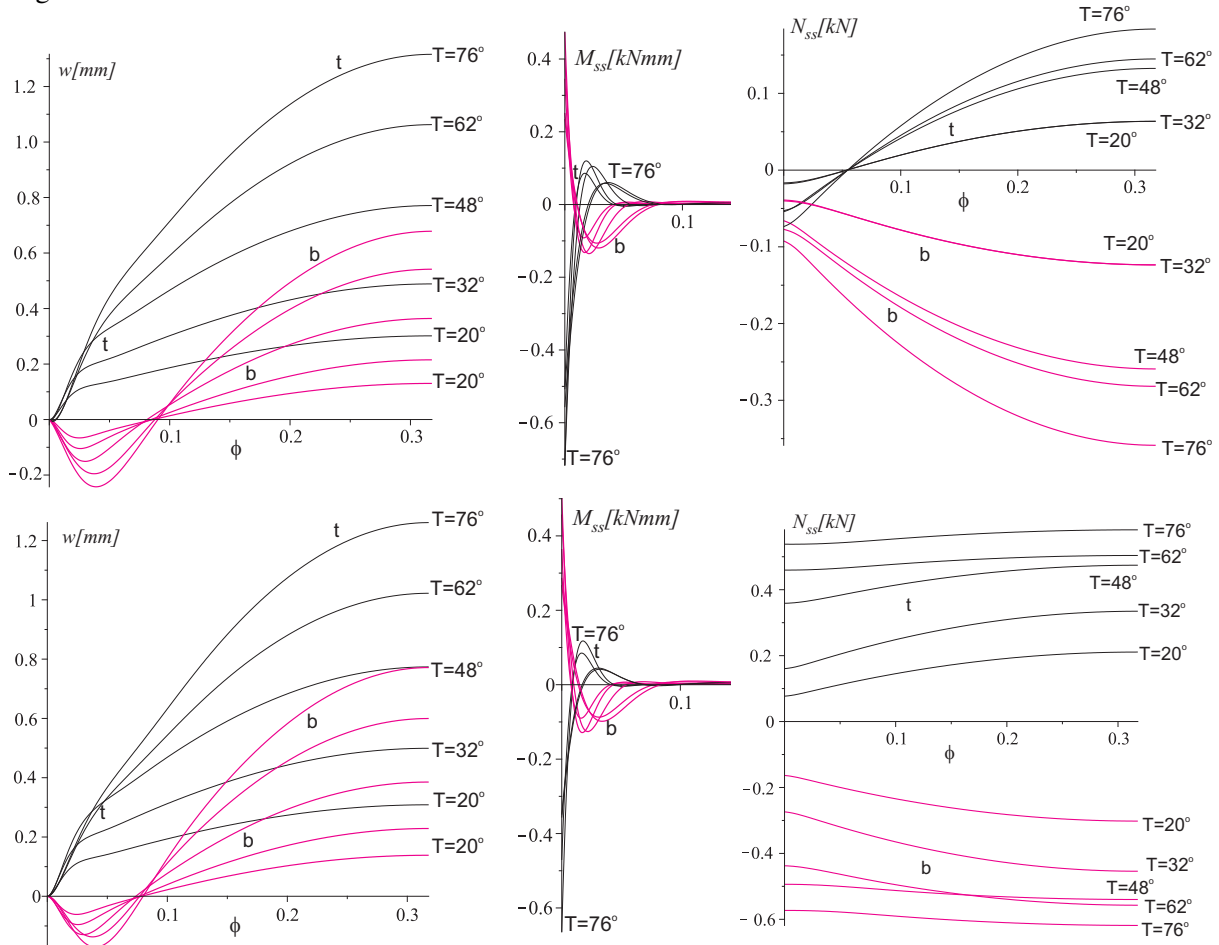


Figure 18. Uniform *thermal loading* results for face sheets along the panel circumference for simply supported (top) and clamped (bottom) systems with *temperature-dependent core properties*. The horizontal coordinate is ϕ ; temperatures in degrees Celsius. Left column: vertical displacements. Middle column: bending moments. Right column: In-plane stress resultant (in core). Thinner black lines marked “t” stand for the upper face or interface; thicker, pink lines marked “b”, for the lower.

The predictions for the face sheets along half of the panel circumference at different temperature levels for the two supporting systems appear in Figure 18. The vertical displacements (Figure 18a) and the bending moments (Figure 18b) of the two supporting systems are almost identical. Also here (see Figure 10 for comparison) the bending moments exist only in the vicinity of the support as a result of the existence of the edge beam. The in-plane stress resultants (Figure 18c) reveal different patterns for the two supporting systems. In the simply supported case the stress resultants of the two face sheets are in compression at near and at the support, and this changes into tension in the upper face sheet and compression in the bottom face sheet away from the supporting region. In the clamped case the upper face sheet is in tension while the lower face sheet is in compression throughout of the length/circumference of

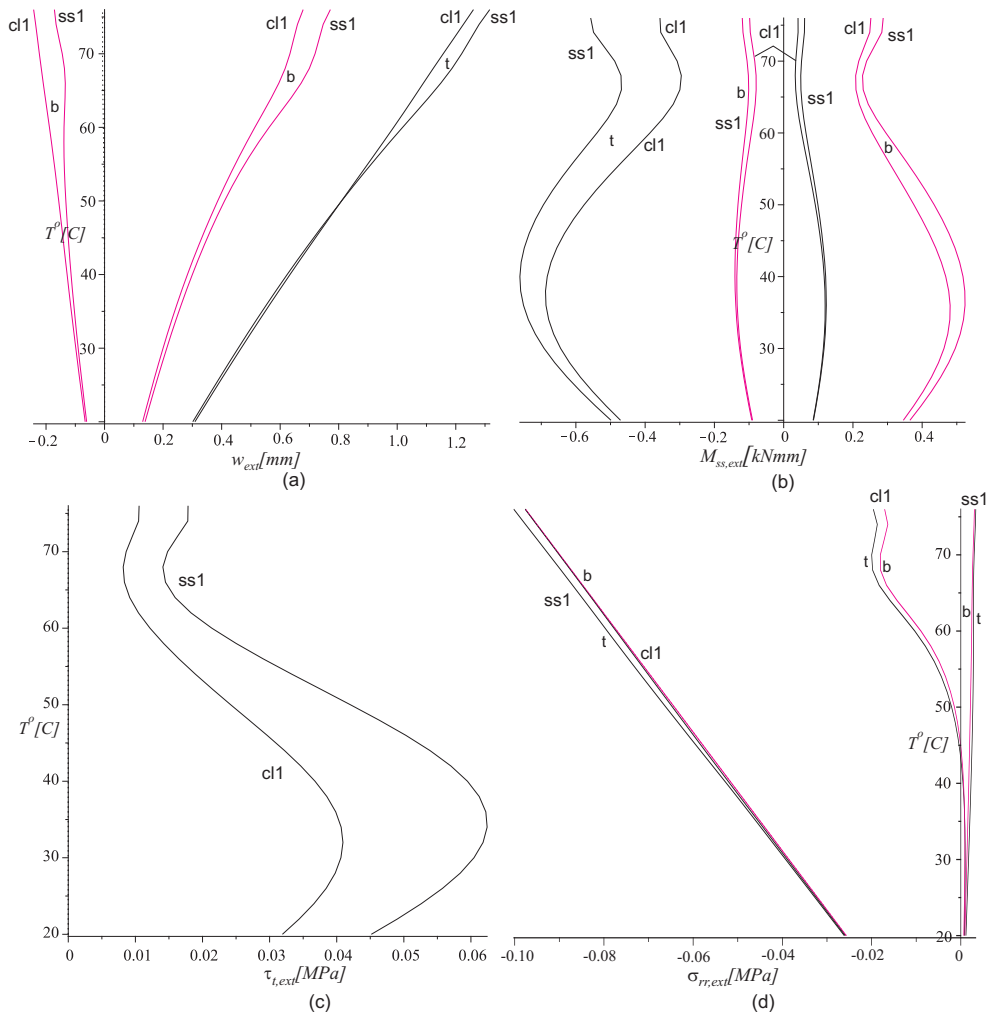


Figure 19. Equilibrium curves of load versus extreme values of (a) vertical displacements of faces sheets, (b) bending moments in faces, (c) shear stress in core, and (d) interfacial radial normal stresses at face-core interfaces, all for curved sandwich panel with *temperature-dependent core properties*, subjected to uniform *thermal loading*. Thin black lines refer to the upper face sheet; thicker pink lines to the lower one.

the panel. The results are very similar to the results obtained for the curved sandwich panel temperature-independent mechanical properties, shown in Figure 10, except for the opposite signs due to the cooling temperatures considered for this example.

The equilibrium curves of temperatures versus extreme values of selected structural quantities for the two supporting systems appear in Figure 19. They reveal a nonlinear behavior which is due to the nonlinearities in the mechanical properties as a result of their temperature dependence. In addition, there are only minor differences between the results of the two supporting systems. The vertical displacement curves (Figure 19a) are almost linear, but they become nonlinear at the upper range of temperatures. The bending moment results (Figure 19b) reveal a nonlinear response in both positive and negative bending moments. The interfacial shear stress results at the upper face core interface (Figure 19c) also reveal a nonlinear response through the range of temperatures. The interfacial radial normal stresses curves, at the upper and lower face core interfaces (Figure 19d) reveal a linear response for the simply supported case and a nonlinear for the clamped case. In both cases the maximum compressive stresses occur in the edge of the panel. However, for the simply supported case there are tensile stresses in the vicinity of the support that do not exist in the clamped system.

Thermomechanical loading. The combined thermal and mechanical loading response study outlines the behavior of the curved sandwich panel when subjected to a concentrated or distributed load below the limit point load levels (see Figures 6 and 8). Again two supporting systems are considered, and the imposed heating temperatures profile change from 20°C to 78°C with and without a gradient between the two face sheets.

We first consider the effects of the thermal degradation of core properties on the response of the simply supported uniformly heated panel with a concentrated load applied at mid-span. The concentrated load is taken as 2.1 kN, which is about 80% of the limit point load without thermal loading (see Figure 6).

The deformed shapes of the panel appear in Figure 20, which reveals an indentation that grows as the temperature is raised. Note here that the thermal loading causes upwards displacements (compare Figure 17), and that the combined thermal and mechanical response yields large indentations as a result of the degrading mechanical core properties.

The vertical displacements along half the circumference of the sandwich panel appear in Figure 21a, where it is observed that quite large values are obtained as the limit point temperature level is reached around $T = 27^\circ\text{C}$ (see Figure 22a). Due to the concentrated load the initial displacement is quite large. The bending moment diagrams (Figure 21b) follow the same trends as obtained when temperature-independent core properties are assumed (see Figure 13), namely, large bending stresses are accumulated in the vicinity of the supports and the load application point. The interfacial shear stresses at the upper

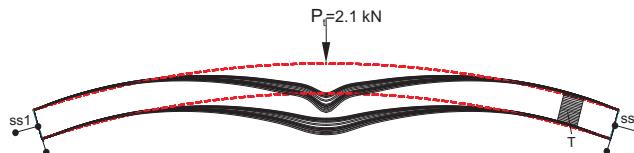


Figure 20. Deformed shapes of the simply supported curved panel subjected to a *concentrated mechanical load* and uniform *thermal loading*, assuming *temperature-dependent core properties*.

and lower face-core interfaces appear in Figure 21c and reveal an attenuation of stresses in the vicinity of the load and the support is observed. The interfacial normal stresses at the top and bottom face-core interfaces (Figure 21d) follow the same trends as found for the bending moments.

The equilibrium curves of temperature versus extreme structural quantities for three loads that lie below the limit point load level when no thermal loading is applied (see Figure 6) appear in Figure 22 for a simply supported curved sandwich panel. In all cases a limit point behavior is observed, and great numerical difficulties that prevent convergence of the solution are encountered.

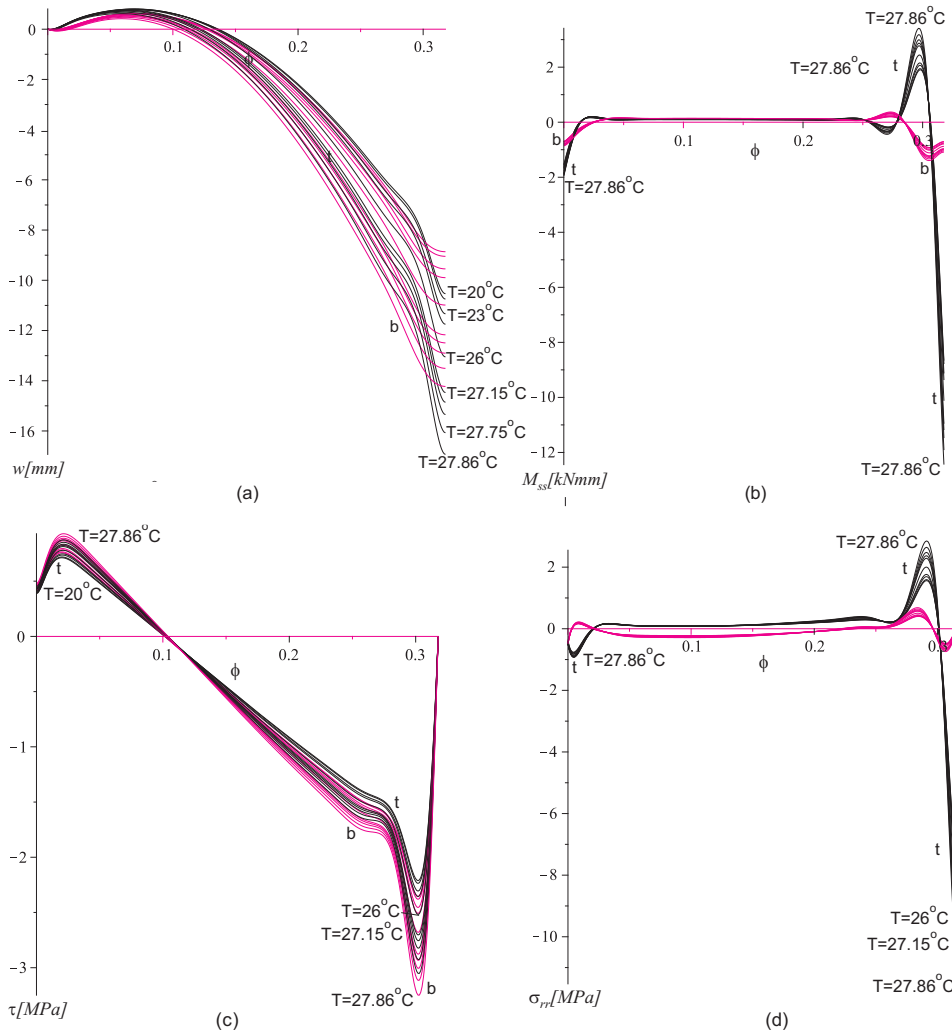


Figure 21. Thermomechanical response results for face sheets along the panel circumference for simply supported panel with *temperature-dependent core properties* when subjected to *concentrated mechanical loading* at mid-span of upper face sheet: (a) vertical displacements, (b) bending moments, (c) shear stresses in face-core interfaces, and (d) radial normal stresses in same. Thinner black lines marked “t” stand for the upper face or interface; thicker, pink lines marked “b”, for the lower.

The temperature versus the vertical displacements curves appear in Figure 22a and they reveal that for the low load level of $P_t = 1.1$ kN the temperature limit point occurs at a temperature of 45.4°C , while for the second load of $P_t = 1.6$ kN the temperature limit point occurs at 37.5°C , and at the higher load of 2.1 kN the critical temperature occurs at 27.86°C . At all load levels the temperature limit point is associated with a zero slope. The bending moment curves (Figure 22b) follow similar trends, but the slope is not zero at the temperature limit point levels. Similar trends are observed in the interfacial shear stresses at the upper face-core interface (Figure 22c) and the interfacial radial (through-the-thickness) normal stresses (Figure 22d).

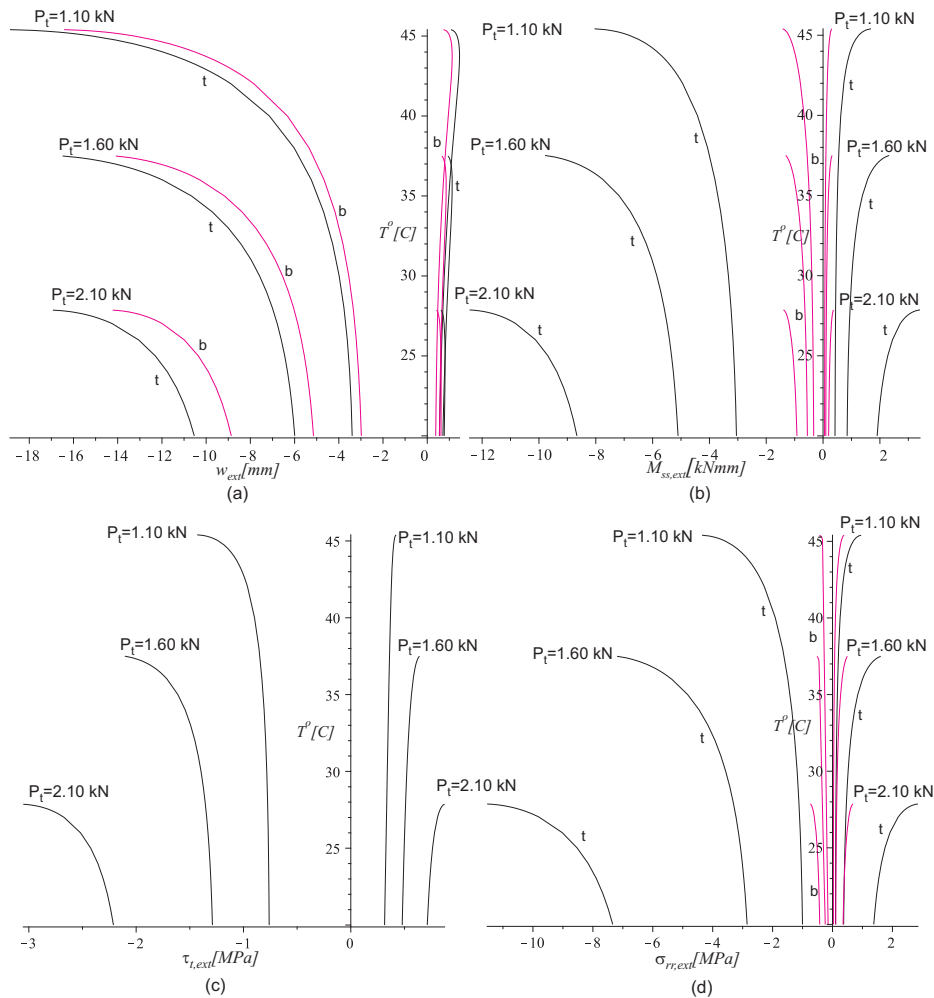


Figure 22. Equilibrium curves of load versus extreme values of (a) vertical displacements of faces sheets, (b) bending moments in faces, (c) shear stress in core, and (d) interfacial radial normal stresses at face-core interfaces, all for simply supported curved sandwich panel with *temperature-dependent core properties*, subjected to various *concentrated mechanical loads*. Thin black lines refer to the upper face sheet; thicker pink lines to the lower one.

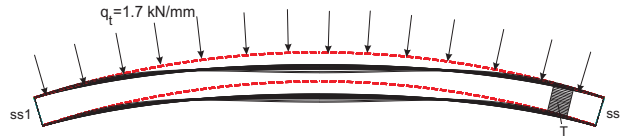


Figure 23. Deformed shapes of the simply supported curved panel when loaded by a fully *distributed mechanical load*, assuming *temperature-dependent core properties*.

The combined thermomechanical response of a simply supported curved sandwich panel with a 1.7 kN/mm distributed load, which is about 90% of the corresponding limit point load level (with no thermal loading), and thermal loadings, at different temperature levels is discussed next. The deformed shapes appear in Figure 23, and reveal quite small deformations (in comparison with the case of a concentrated load) with smooth displacements patterns and no signs of local buckling as observed in the case of temperature-independent properties (see Figure 7).

The vertical displacements of the face sheets along half the circumference of the panel appear in Figure 24a, where a significant growth of the displacements at the limit point temperature level of 27.72°C is observed. The bending moment diagrams reveal a ripple type patterns in the vicinity of the supports (Figure 24b). The interfacial shear stresses at the upper and lower face-core interfaces (Figure 24c) yield significant values in the vicinity of the edge as well at the quarter of the circumference/span. The trends of the interfacial radial normal stresses (Figure 24d) follow the same trends as those of the bending moments.

The effects of the magnitude of the distributed load level on the equilibrium curves of the combined thermomechanical response of a simply supported curved panel are described in Figure 25. The temperature versus the extreme values of the vertical displacements of the face sheet curves for the different load levels appear in Figure 25a. At all load levels a limit point behavior is detected, and the temperature at which the limit point is reached is lowered as the magnitude of the distributed load is increased. Also, here, the slope of the curves at the limit point approaches zero. Note here that up to the limit point temperature the displacements almost do not change with respect to the initial level (zero temperature), while in the near vicinity of the limit point temperature there is a significant change (increase) of the displacements. With respect to the bending moment curves for the face sheets (Figure 25b) and the curved of the interfacial radial normal stresses at the face-core interfaces (Figure 25d) there is a gradual change between the initial values (no thermal loading) and those at the limit point. With respect to the interfacial shear stresses at the upper face-core interface (Figure 25c) the values prior to the limit point reduce and they are significantly increased at the limit point temperature level.

The effects of a gradient in temperature between the upper and lower face sheets appear in Figures 26 and 27, where the high temperature is at the lower face sheet. The combined thermomechanical response of the simply supported and clamped curved sandwich panels includes, in addition to the thermal loading, a concentrated and a distributed load.

The equilibrium curves of the combined thermomechanical response of a concentrated load that is applied at the mid-span of the upper face sheet appear in Figure 26. The results include curves for temperature versus some extreme values of selected structural quantities for the two supporting systems and with a radial thermal gradient across the core thickness between zero to 40°C. The applied loads are 1.1 kN for the simply supported and 1.4 kN for the clamped panel. Both loads are far below the limit

load level with no thermal loading (see Figure 6). The vertical displacement curves of the face sheets appear in Figure 26, top. For the case of a simply supported sandwich panel the response is described by a limit point with almost zero slope at the limit point (Figure 26, top left), which represents an unstable behavior. However, for the clamped case (Figure 26, top right) the curves represent a stable behavior for the low gradients and less stable for the higher gradients (possibly converging towards unstable behavior for very large thermal gradients). The differences between the results of the two supporting systems are much more significant when studying the bending moments curves (see middle row in Figure 26).

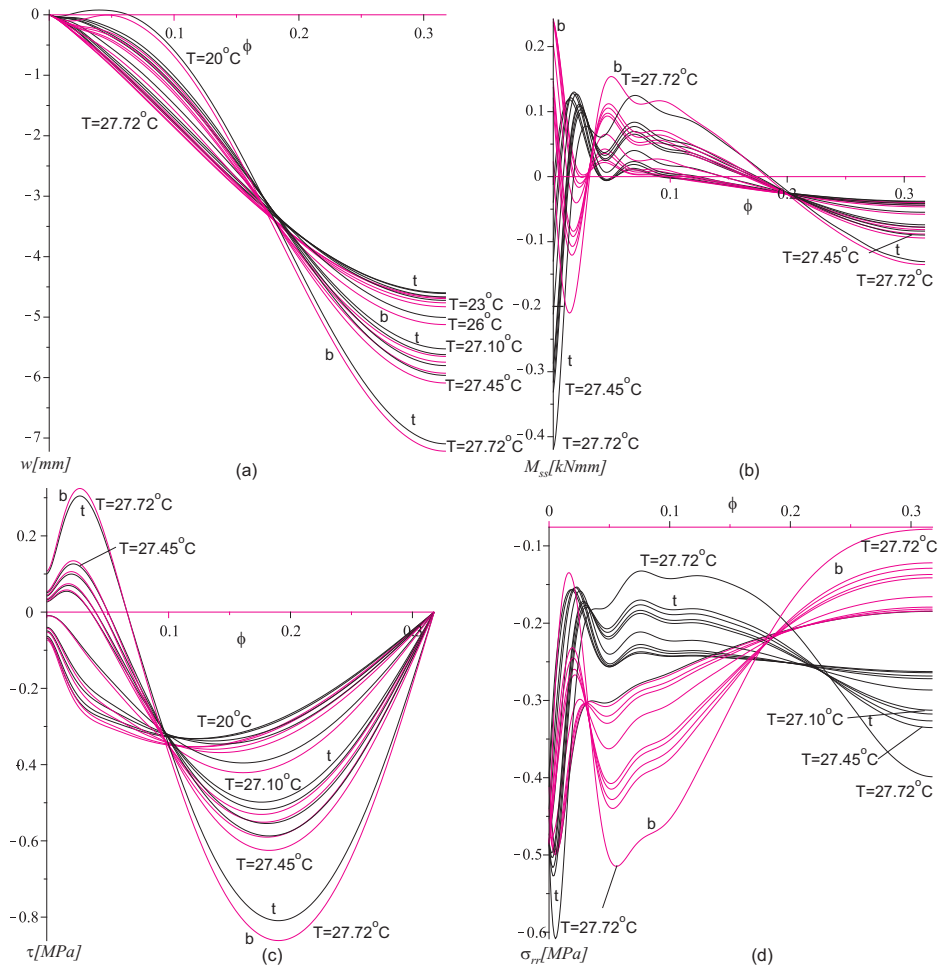


Figure 24. Thermomechanical response results for face sheets along the panel circumference for simply supported panel with *temperature-dependent core properties* when subjected to a fully *distributed mechanical load* applied on upper face sheet and uniform *temperature loading*. Temperatures are in degrees Celsius. Shown are (a) vertical displacements, (b) bending moments, (c) shear stresses in face-core interfaces, and (d) radial normal stresses in same. Thinner black lines marked “t” stand for the upper face or interface; thicker, pink lines marked “b”, for the lower.

The interfacial radial normal stresses (Figure 26, bottom) follow the same trends as those of the bending moments. It should be noticed that in all cases the clamped support conditions yields a more stable behavior as compared with the simply supported sandwich panel.

The combined thermomechanical response for the case of distributed mechanical loads with a thermal gradient between the lower and the upper face sheets appears in Figure 27. Here, the distributed load equals 1.7 kN/mm for the both supporting systems. The equilibrium curves reveal, in all figures, that the differences between the simply supported panel and clamped are minor. Moreover, the equilibrium curves show that responses are generally unstable for any value of the thermal gradient value. The

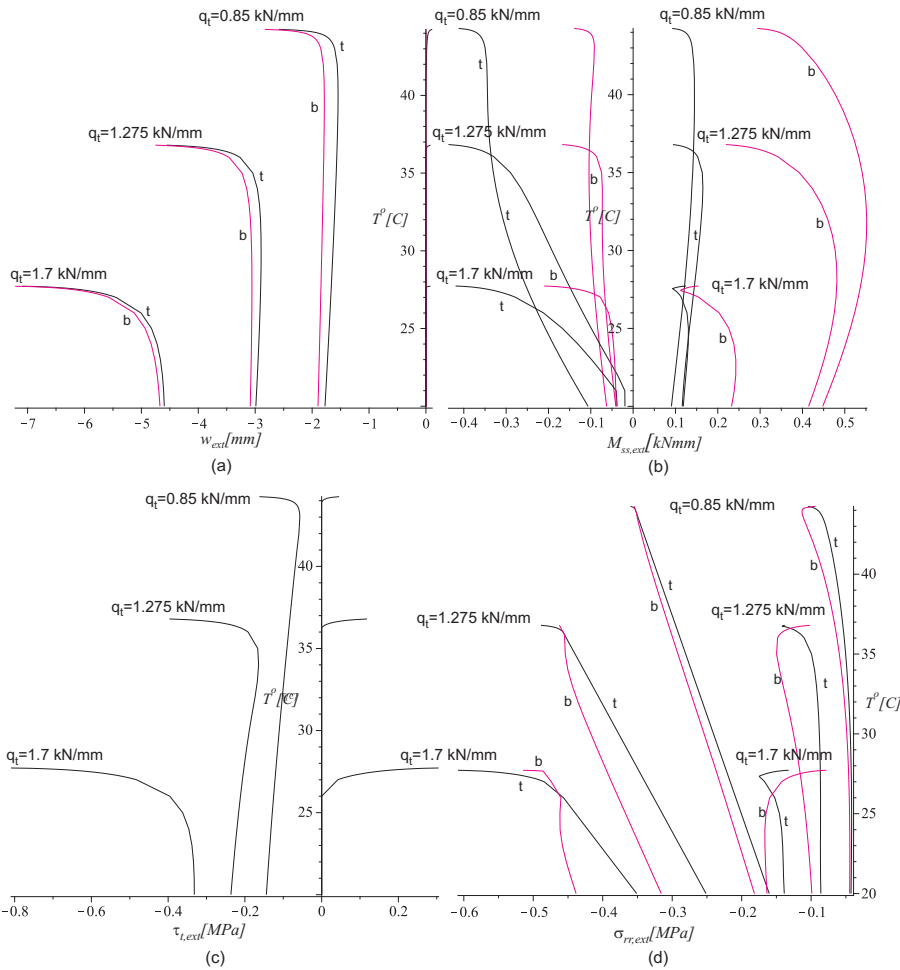


Figure 25. Equilibrium curves of load versus extreme values of (a) vertical displacements of faces sheets, (b) bending moments in faces, (c) shear stress in core, and (d) interfacial radial normal stresses at face-core interfaces, all for simply supported curved sandwich panel with *temperature-dependent core properties*, subjected to a *distributed mechanical load* applied at the upper face sheet and uniform *temperature loading*. Thin black lines refer to the upper face sheet; thicker pink lines to the lower one.

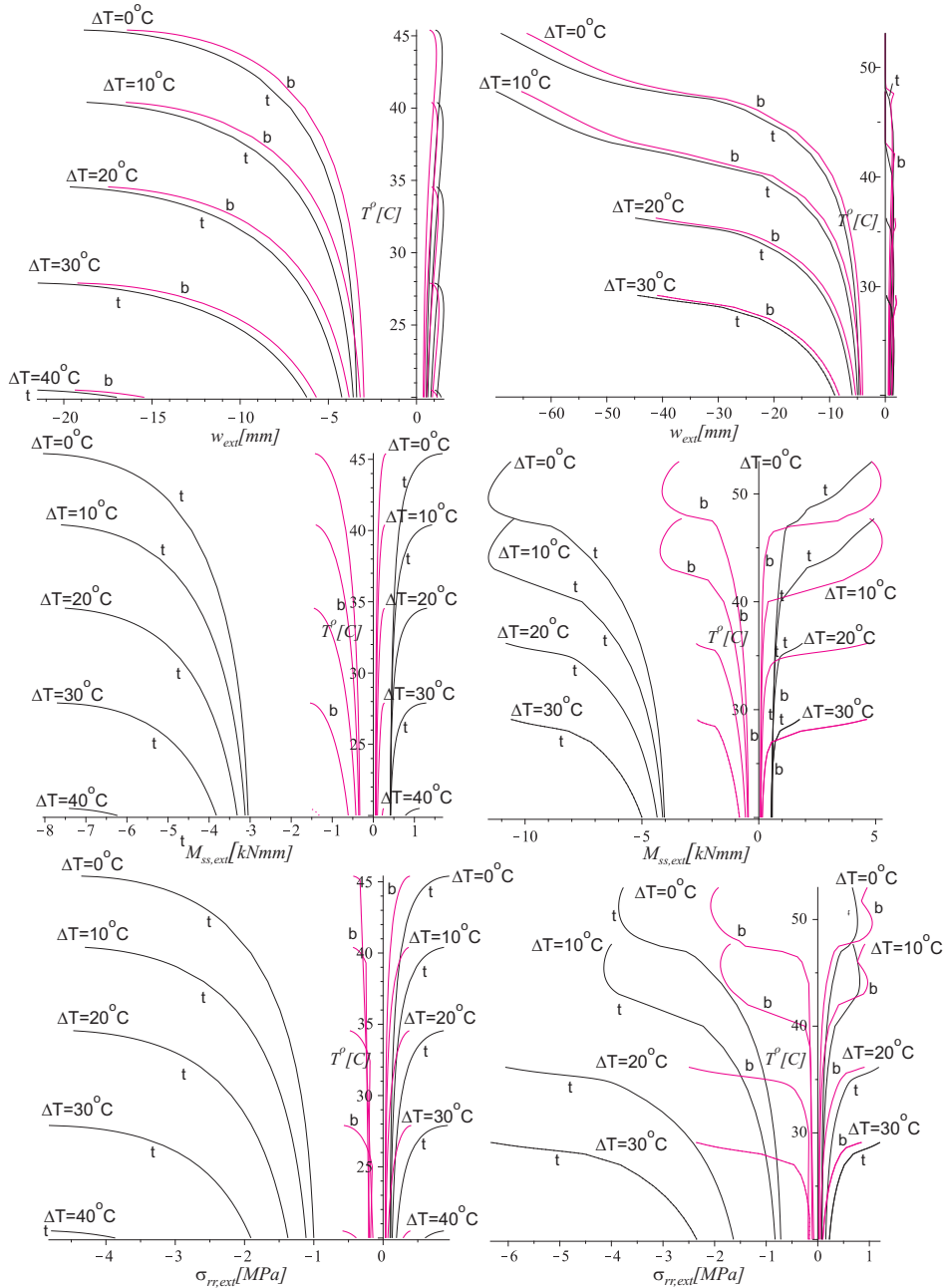


Figure 26. Equilibrium curves of load versus extreme values of vertical displacements of face sheets (top), bending moments in faces (middle), and interfacial radial normal stresses at face-core interfaces (bottom), all for simply supported (left, $P_a = 1.1$ kN) and clamped (right, $P_a = 1.4$ kN) curved sandwich panels with *temperature-dependent core properties*, subjected to a *concentrated mechanical load* P_a applied at mid-span of upper face sheet and *thermal loading* with different *through-the-thickness gradients*. Thin black lines refer to the upper face sheet; thicker pink lines to the lower one.

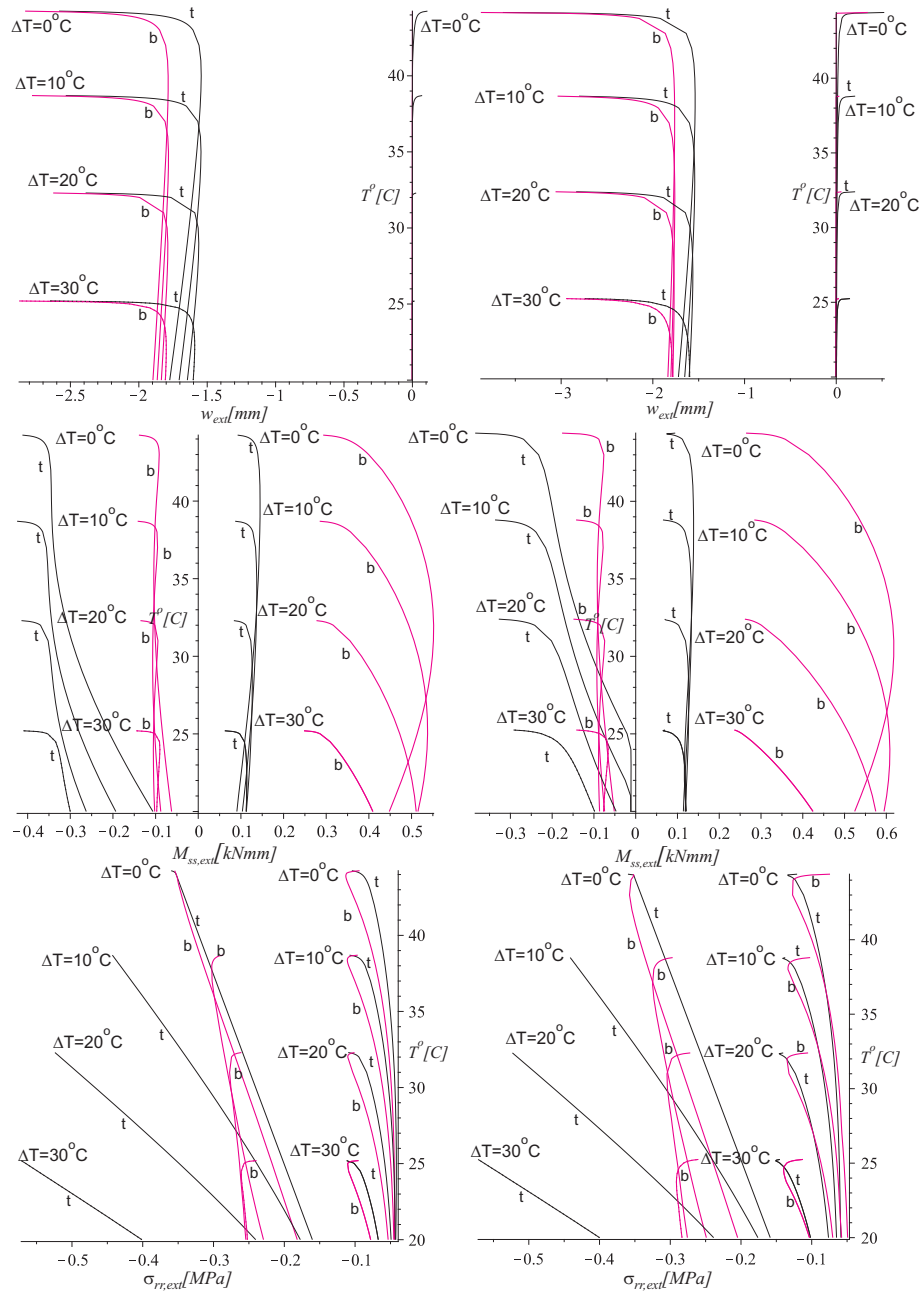


Figure 27. Equilibrium curves of load versus extreme values of vertical displacements of face sheets (top), bending moments in faces (middle), and interfacial radial normal stresses at face-core interfaces (bottom), all for simply supported (left) and clamped (right) curved sandwich panels with *temperature-dependent core properties*, subjected to a *distributed mechanical load* of 0.85 kN/mm applied to upper face sheet and *thermal loading* with different *through-the-thickness gradients*. Thin black lines refer to the upper face sheet; thicker pink lines to the lower one.

curves of extreme values of the vertical displacements of the face sheets versus temperature (Figure 27, top) yield a limit point behavior with a slope of almost zero for both supporting systems. Here it should be noticed that for both cases significant changes of the displacements occur only in the near vicinity of the limit point temperature level. The bending moment curves (Figure 27, middle row) reveal similar trends, with the exception that there is a gradual change between the initial values (corresponding to no thermal loading) and moment values at the limit point. Notice that the negative bending moments of the clamped case are smaller than those of the simply supported case and vice versa with respect to the positive bending moments. The relationship between the radial interfacial normal stresses and the temperature (Figure 27, bottom) is almost linear for the extreme values of the compressive stresses at the upper interface and nonlinear at the lower interface for both supporting systems.

6. Summary and conclusions

The geometrically nonlinear behavior of curved sandwich panels subjected to thermal and mechanical loading was studied, under both temperature-independent (TI) and temperature-dependent (TD) assumptions for the core material properties.

The first half of the paper gives a mathematical formulation for the TI case, based on a variational approach along with high-order sandwich panel theory (HSAPT). The analysis considers the thermal strains of the core along with the effects of its flexibility in the radial (through-the-thickness) direction. The nonlinear field equations of the curved sandwich panel are derived along with the appropriate boundary conditions. The effects of a solid edge beam at the edge of the curved sandwich panel on the boundary conditions are considered. The stress and displacement fields of the core are derived and solved explicitly for the case of a core with uniform mechanical properties. The full nonlinear governing equations are derived and presented.

The second half models thermally induced deformations of curved sandwich panels using the equations previously obtained via HSAPT. The stress and displacement fields of the core are derived and solved explicitly for cores with both TI and TD mechanical properties. The solution for a core with mechanical properties dependent on the radial coordinate is derived and is used to handle the TD case. A polynomial solution is adopted, and a general solution is presented for the stress and displacement fields. The nonlinear response is determined through the solution of the nonlinear equations using a finite-difference scheme along with a natural parametric continuation or a pseudo-arclength or similar procedure.

A numerical study then investigates the response of a shallow curved sandwich panel with a geometry that has been used previously in an experimental study conducted at Aalborg University. The shallow curved sandwich panel is assumed to be subjected to a concentrated or fully distributed load in addition to thermal loading. The panel consists of two aluminum face sheets and a cross-linked PVC H60 Divinicell foam core with mechanical properties that degrade with increasing temperature. The loading system consists of an edge beam at the edges of the curved sandwich panel, resting on a simply supported or clamped system with immovable conditions in the radial direction. The thermal loading consists of heating and cooling temperatures that are uniformly distributed circumferentially, with or without a gradient through the depth of the panel.

The numerical study covers all the combinations of the mechanical-thermal response with TI core properties. The response due to purely mechanical loading is presented first and reveals a typical limit

point behavior for both supporting systems and both types of loads. The study further reveals that under a concentrated load, there is an ascending branch beyond the limit point for the case of a simply supported system. For the case of a distributed load the nonlinear responses are almost identical for the two supporting systems, with insignificant differences in the limit-point load level. For this case local buckling of the upper face sheet is observed for both supporting systems, in addition to local buckling of the lower face sheet in the vicinity of the support when the sandwich panel is clamped at the edges.

Thermal loading with temperature-independent core properties reveals that the response is linear through the entire range from (subzero) cooling to (elevated) heating temperatures, with either uniform or gradient-type distributions through the depth of the sandwich panel. For case of heating the panel expands and changes its circumferential length rather than causing compression, as observed with flat panels. Hence, heating improves the performance of the loaded sandwich panel, since it cancels part of the induced deformations and stresses due to mechanical loading. In the case of cooling the panel contracts, yielding displacements and stress fields similar to those of the mechanical loads.

The thermomechanical response is determined for a mechanical load that is below the limit-point load level where the thermal loading changes from heating to cooling temperatures. For the case of heating, or loads below 85% of the mechanical limit point load, the response is linear for all loading cases and supporting systems. For loads in the range of 90% of the mechanical limit load, the thermomechanical response is nonlinear for the simply supported system for both types of loads. For the case of the clamped supporting system the concentrated load does not yield a limit point within the range of temperatures considered, while for the case of the distributed load a limit point is observed.

The combined response of a distributed load along with cooling temperatures yields a limit point response that is associated with local buckling ripples around mid-span of the upper face sheet and local buckling at the lower face at the support when it is clamped.

The characteristics of the combined response under TI mechanical properties of the core resemble those of the case with mechanical loads only when a limit point behavior is observed. Thus, the thermomechanical response for a curved sandwich panel subjected to both concentrated mechanical load and a thermal load yields similar characteristics to those of case when only a concentrated mechanical load is applied. Hence, the combined mode is actually a nonlinear combination of the mechanical and the thermal loads, and any combination of the two, in terms of magnitude, can yield a response that resembles that obtained for the case when only a mechanical load is applied.

The thermal loading case when the core properties are assumed to be TD follows the same trends as those encountered for the TI case. However, the equilibrium curves of temperature versus extreme values of selected structural quantities are generally nonlinear, due to the nonlinear change of the mechanical core properties with increasing temperature. The effect of the supporting system is minor.

The combined thermomechanical response with TD properties is quite different from that of the TI case and is associated with a limit point behavior at low temperature values. For the TI case only thermal loading in the form of cooling yields a nonlinear responses that are associated with limit point behavior. However, for the TD case the degradation of the core properties governs and yields nonlinear responses with unstable limit point behavior, even though the stress and displacement fields induced by the thermal loads act opposite to those induced by the mechanical loads.

The effects of the load level on the combined thermomechanical response have been investigated for loads below the limit point level for pure mechanical loading case. For the case of a concentrated load,

the response of a simply supported curved sandwich panel is associated with a limit point behavior which is unstable, while that obtained for the clamped case yields a stable behavior that resembles that of a plate sandwich panel structure. Generally, as the load is increased the limit point temperature reduces. For the case of a fully distributed load both the simply supported and the clamped sandwich panels yield unstable limit point responses with very similar limit point temperature values as a result of initiation of local buckling in the compressed face sheet.

For the case where the highest (heated) temperature is on the lower tensile face sheet an unstable limit point behavior of the simply supported panel is observed as the gradient increases, whereas a stable response is obtained for the clamped panel when a concentrated load is considered. For the case of a uniform distributed load an unstable limit point response is observed for both supporting systems with almost identical limit point temperature values. In all cases, an increase of the thermal gradient is associated with a reduction of the limit point temperature.

Acknowledgement

This work was conducted while Frostig was a visiting professor at the Institute of Mechanical Engineering at Aalborg University. The visiting professorship and the research presented herein were sponsored by the US Navy, Office of Naval Research (ONR), Award N000140710227 (“Influence of local effects in sandwich structures under general loading conditions and ballistic impact on advanced composite and sandwich structures”, program manager Dr. Yapa D. S. Rajapakse) and by the Ashtrom Engineering Company, which supports Frostig’s professorship chair at his home institution. The financial support received is gratefully acknowledged. Special thanks to Silvio Levy, the journal’s technical editor, for his accurate and superb work.

References

- [Ascher and Petzold 1998] U. M. Ascher and L. Petzold, *Computer methods for ordinary differential equations and differential-algebraic equations*, SIAM, Philadelphia, 1998.
- [Bozhevolnaya 1998] E. Bozhevolnaya, *A theoretical and experimental study of shallow sandwich panels*, Ph.D. thesis, Institute of Mechanical Engineering, Aalborg University, Aalborg, 1998. Supervisor: A. Kildegaard.
- [Bozhevolnaya and Frostig 1997] E. Bozhevolnaya and Y. Frostig, “Nonlinear closed-form high-order analysis of curved sandwich panels”, *Compos. Struct.* **38**:1–4 (1997), 383–394.
- [Bozhevolnaya and Frostig 2001] E. Bozhevolnaya and Y. Frostig, “Free vibrations of curved sandwich beams with a transversely flexible core”, *J. Sandw. Struct. Mater.* **3**:4 (2001), 311–342.
- [Brush and Almroth 1975] D. O. Brush and B. O. Almroth, *Buckling of bars, plates and shells*, McGraw-Hill, New York, 1975.
- [Burmam 2005a] M. Burmann, “Testing of compressive properties of Divinycell P and HP grades under elevated temperatures”, Department of Aeronautical and Vehicle Engineering, Royal Institute of Technology, 2005, Stockholm. Test Protocol, C2005-05.
- [Burmam 2005b] M. Burmann, “Testing of shear properties of Divinycell P and HP grades under elevated temperatures”, Department of Aeronautical and Vehicle Engineering, Royal Institute of Technology, 2005, Stockholm. Test Protocol, C2005-10.
- [DIAB 2003] DIAB, “Data sheets for Divinycell cross-linked PVC foams”, www.diabgroup.com, 2003.
- [Fernlund 2005] G. Fernlund, “Spring-in angled sandwich panels”, *Compos. Sci. Technol.* **65**:2 (2005), 317–323.
- [Frostig 1999] Y. Frostig, “Bending of curved sandwich panels with a transversely flexible core: closed-form high-order theory”, *J. Sandw. Struct. Mater.* **1**:1 (1999), 4–41.

- [Frostig and Thomsen 2007] Y. Frostig and O. T. Thomsen, "Buckling and nonlinear response of sandwich panels with a compliant core and temperature-dependent mechanical properties", *J. Mech. Mater. Struct.* **2**:7 (2007), 1355–1380.
- [Frostig and Thomsen 2008a] Y. Frostig and O. T. Thomsen, "Thermal buckling and postbuckling of sandwich panels with a transversely flexible core", *AIAA J.* **46**:8 (2008), 1976–1989.
- [Frostig and Thomsen 2008b] Y. Frostig and O. T. Thomsen, "Non-linear thermal response of sandwich panels with a flexible core and temperature dependent mechanical properties", *Compos. B Eng.* **39**:1 (2008), 165–184.
- [Frostig et al. 1992] Y. Frostig, M. Baruch, O. Vilnay, and I. Sheinman, "High-order theory for sandwich-beam bending with transversely flexible core", *J. Eng. Mech. (ASCE)* **118**:5 (1992), 1026–1043.
- [Hentinen and Hildebrand 1991] M. Hentinen and M. Hildebrand, "Nonlinear behavior of single-skin and sandwich hull panels", pp. 1039–1063 in *FAST '91: First International Conference on Fast Sea Transportation* (Trondheim, 1991), vol. 2, edited by K. O. Holden et al., Tapir, Trondheim, 1991.
- [Hildebrand 1991] M. Hildebrand, *On the bending and transverse shearing behaviour of curved sandwich panels*, VTT Tiedoteita - Research Notes **1249**, Valtion Teknillinen Tutkimuskeskus, Espoo, 1991.
- [Kant and Kommineni 1992] T. Kant and J. R. Kommineni, "Geometrically non-linear analysis of doubly curved laminated and sandwich fibre reinforced composite shells with a higher order theory and C^0 finite elements", *J. Reinf. Plast. Compos.* **11**:9 (1992), 1048–1076.
- [Karayadi 1998] E. Karayadi, *Collapse behavior of imperfect sandwich cylindrical shells*, Ph.D. thesis, Delft University of Technology, Faculty of Aerospace Engineering, Delft, 1998. Supervisor: A. Arbocz.
- [Keller 1992] H. B. Keller, *Numerical methods for two-point boundary value problems*, Dover, New York, 1992.
- [Ko 1999] W. L. Ko, "Open-mode debonding analysis of curved sandwich panels subjected to heating and cryogenic cooling on opposite faces", NASA Technical Publication NASA/TP-1999-206580, Dryden Flight Research Center, Edwards, CA, June 1999, Available at <http://dtrs.dfrc.nasa.gov/archive/00000090>.
- [Kollár 1990] L. P. Kollár, "Buckling of generally anisotropic shallow sandwich shells", *J. Reinf. Plast. Compos.* **9**:6 (1990), 549–568.
- [Kühhorn and Schoop 1992] A. Kühhorn and H. Schoop, "A nonlinear theory for sandwich shells including the wrinkling phenomenon", *Arch. Appl. Mech.* **62**:6 (1992), 413–427.
- [Librescu and Hause 2000] L. Librescu and T. Hause, "Recent developments in the modeling and behavior of advanced sandwich constructions: a survey", *Compos. Struct.* **48**:1–3 (2000), 1–17.
- [Librescu et al. 1994] L. Librescu, W. Lin, M. P. Nemeth, and J. H. Starnes, Jr., "Effects of tangential edge constraints on the postbuckling behavior of flat and curved panels subjected to thermal and mechanical loads", pp. 55–71 in *Buckling and postbuckling of composite structures: proceedings of the 1994 International Mechanical Engineering Congress* (Chicago, 1994), edited by A. K. Noor, Aerospace Division **41**, ASME, New York, 1994. NASA-TM-111522.
- [Librescu et al. 2000] L. Librescu, M. P. Nemeth, J. H. Starnes, Jr., and W. Lin, "Nonlinear response of flat and curved panels subjected to thermomechanical loads", *J. Therm. Stresses* **23**:6 (2000), 549–582.
- [Lo et al. 1977] K. H. Lo, R. M. Christensen, and E. M. Wu, "A high-order theory of plate deformation", *J. Appl. Mech. (ASME)* **44** (1977), 669–676.
- [Noor and Burton 1990] A. K. Noor and W. S. Burton, "Assessment of computational models for multilayered anisotropic plates", *Compos. Struct.* **14**:3 (1990), 233–265.
- [Noor et al. 1994] A. K. Noor, W. S. Burton, and J. M. Peters, "Hierarchical adaptive modeling of structural sandwiches and multilayered composite panels", *Appl. Numer. Math.* **14**:1–3 (1994), 69–90.
- [Noor et al. 1996] A. K. Noor, W. S. Burton, and C. W. Bert, "Computational models for sandwich panels and shells", *Appl. Mech. Rev. (ASME)* **49**:3 (1996), 155–199.
- [Noor et al. 1997] A. K. Noor, J. H. Starnes, Jr., and J. M. Peters, "Curved sandwich panels subjected to temperature gradient and mechanical loads", *J. Aerosp. Eng. (ASCE)* **10**:4 (1997), 143–161.
- [Rao 1985] K. M. Rao, "Buckling analysis of FRP-faced anisotropic cylindrical sandwich panel", *J. Eng. Mech. (ASCE)* **111**:4 (1985), 529–544.

- [Rao and Meyer-Piening 1986] K. M. Rao and H. R. Meyer-Piening, "Critical shear loading of curved sandwich panels faced with fiber-reinforced plastic", *AIAA J.* **24**:9 (1986), 1531–1536.
- [Rao and Meyer-Piening 1990] K. M. Rao and H. R. Meyer-Piening, "Buckling analysis of FRP faced cylindrical sandwich panel under combined loading", *Compos. Struct.* **14**:1 (1990), 15–34.
- [Reddy 1984a] J. N. Reddy, "A simple higher-order theory for laminated composite shells", *J. Appl. Mech. (ASME)* **51**:4 (1984), 745–752.
- [Reddy 1984b] J. N. Reddy, "Exact solutions of moderately thick laminated shells", *J. Eng. Mech. (ASCE)* **110**:5 (1984), 794–809.
- [di Sciuva 1987] M. di Sciuva, "An improved shear-deformation theory for moderately thick multilayered anisotropic shells and plates", *J. Appl. Mech. (ASME)* **54**:3 (1987), 589–596.
- [di Sciuva and Carrera 1990] M. di Sciuva and E. Carrera, "Static buckling of moderately thick, anisotropic, laminated and sandwich cylindrical shell panels", *AIAA J.* **28**:10 (1990), 1782–1793.
- [Simitzes 1976] G. J. Simitzes, *An introduction to the elastic stability of structures*, Prentice-Hall, Englewood Cliffs, NJ, 1976.
- [Smidt 1993] S. Smidt, "Curved sandwich beams and panels: theoretical and experimental studies", Report 93-10, Royal Institute of Technology, Stockholm, 1993.
- [Smidt 1995] S. Smidt, "Bending of curved sandwich beams", *Compos. Struct.* **33**:4 (1995), 211–225.
- [Stein 1986] M. Stein, "Nonlinear theory for plates and shells including the effects of transverse shearing", *AIAA J.* **24**:9 (1986), 1537–1544.
- [Stoer and Bulirsch 1980] J. Stoer and R. Bulirsch, *Introduction to numerical analysis*, Springer, New York, 1980.
- [Thomsen and Vinson 2001] O. T. Thomsen and J. R. Vinson, "Analysis and parametric study of non-circular pressurized sandwich fuselage cross section using a high-order sandwich theory formulation", *J. Sandw. Struct. Mater.* **3**:3 (2001), 220–250.
- [Tolf 1983] G. Tolf, "Stresses in a curved laminated beam", *Fibre Sci. Technol.* **19**:4 (1983), 243–267.
- [Vaswani et al. 1988] J. Vaswani, N. T. Asnani, and B. C. Nakra, "Vibration and damping analysis of curved sandwich beams with a viscoelastic core", *Compos. Struct.* **10**:3 (1988), 231–245.
- [Wang and Wang 1989] Y.-J. Wang and Z.-M. Wang, "Nonlinear stability analysis of a sandwich shallow cylindrical panel with orthotropic surfaces", *Appl. Math. Mech.* **10**:12 (1989), 1119–1130.
- [Whitney and Pagano 1970] J. M. Whitney and N. J. Pagano, "Shear deformation in heterogeneous anisotropic plates", *J. Appl. Mech. (ASME)* **37**:4 (1970), 1031–1036.

Received 31 Dec 2008. Revised 3 Jun 2009. Accepted 4 Jun 2009.

YEOSHUA FROSTIG: cvrfros@techunix.technion.ac.il

Professor, Ashtrom Engineering Company Chair in Civil Engineering

Technion - Israel Institute of Technology, Faculty of Civil and Environmental Engineering, Haifa, 32000, Israel

OLE THOMSEN: ott@me.aau.dk

Professor, Head of Department

Aalborg University, Department of Mechanical Engineering, Pontoppidanstræde 105, 9220 Aalborg Ø, Denmark